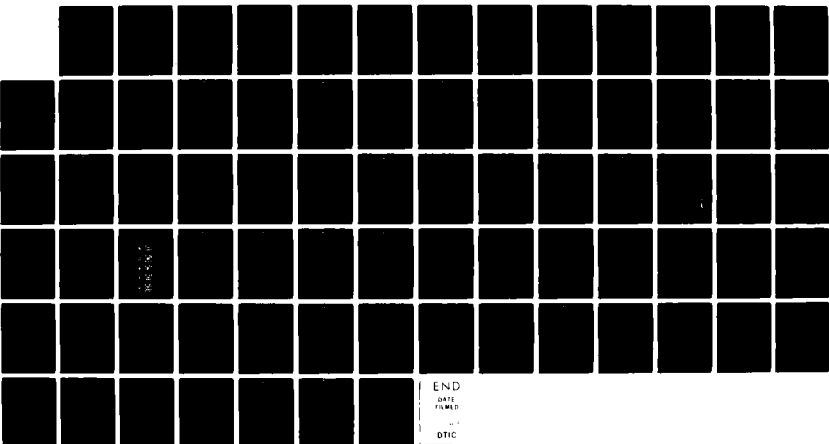
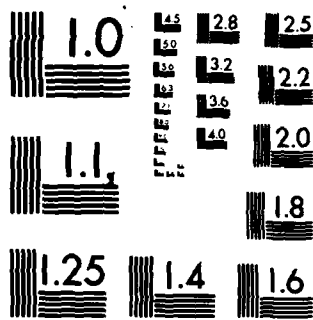


AD-A129 534 ASSESSMENT AND DEVELOPMENT OF OCULOMOTOR FLYING SKILLS 1/1  
BY THE APPLICATION.. (U) DALHOUSIE UNIV HALIFAX (NOVA  
SCOTIA) CENTRE FOR RESEARCH IN S.. D REGAN 22 DEC 82  
UNCLASSIFIED AFOSR-TR-83-0541 AFOSR-78-3711 F/G 5/9 NL



END  
DATE FILMED  
12-1-82  
DTIC



MICROCOPY RESOLUTION TEST CHART  
NATIONAL BUREAU OF STANDARDS 1963-A

| REPORT DOCUMENTATION PAGE   |  |  | READ INSTRUCTIONS BEFORE COMPLETING FORM |
|---|--|--|--|
| 1. REPORT NUMBER<br><b>AFOSR-TR- 83- 0541</b>   | 2. GOVT ACCESSION NO.<br><b>AD-A129534</b> | 3. RECIPIENT'S CATALOG NUMBER  |  |
| 4. TITLE (and Subtitle)<br>Assessment and development of oculomotor flying skills by the application of the channel theory of vision.   |  | 5. TYPE OF REPORT & PERIOD COVERED<br>Final<br>1 Oct 81 - 30 Sept 82                     |  |
| 6. PERFORMING ORG. REPORT NUMBER<br><b>(14)</b><br>D. Regan   |  | 7. CONTRACT OR GRANT NUMBER(s)<br><b>AFOSR-78-3711</b>                                   |  |
| 8. PERFORMING ORGANIZATION NAME AND ADDRESS<br>Centre for Research in Sensory Psychology and Medical Physics, Dalhousie University, Halifax, Nova Scotia, Canada B3J 1B6  |  | 9. PROGRAM ELEMENT, PROJECT, TASK AREA & WORK UNIT NUMBERS<br><b>621102F<br/>2813/A5</b> |  |
| 10. CONTROLLING OFFICE NAME AND ADDRESS<br><b>AFOSR, Bolling AFB, D.C. 20332</b>  |  | 11. REPORT DATE<br><b>22 December 1982</b>   |  |
|   |  | 12. NUMBER OF PAGES<br><b>74f</b>  |  |
| 13. MONITORING AGENCY NAME & ADDRESS (if different from Controlling Office)   |  | 14. SECURITY CLASS. (of this report)<br><b>UNCLASSIFIED</b>                              |  |
|   |  | 15a. DECLASSIFICATION/DOWNGRADING SCHEDULE   |  |
| 16. DISTRIBUTION STATEMENT (of this Report)<br>Approved for public release  |  |  |  |
| 17. DISTRIBUTION ST. AGENT (of if abstract entered in Block 20, if different from Report)<br><b>S ELECTED JUN 20 1983</b>   |  |  |  |
| 18. SUPPLEMENTARY NOTES   |  |  |  |
| 19. KEY WORDS (Continue on reverse side if necessary and identify by block number)<br>Visual flying skills, visual training, visual assessment, visual simulation, vision, motion perception, eye-limb coordination, stereoscopic depth perception, visual contrast sensitivity.  |  |  |  |
| 20. ABSTRACT (Continue on reverse side if necessary and identify by block number)<br>Pilots' landing and formation flight performance on the ASPT simulator correlated with visual sensitivity to an expanding flow pattern and with depth tracking test errors. Pilots who were better able to differentiate different rates of expansion of a test flow pattern achieved a greater percentage of hits and misses in low-level flight and bombing tasks. Aircraft flying grades correlated with flow pattern test results.<br>As stimuli for motion in depth, either texture changes alone or changes in |  |  |  |

FILE COPY

DD FORM 1 JAN 73 1473

83 06 20 002

SECURITY CLASSIFICATION OF THIS PAGE (When Data Entered)

IN CLASS, FILED

**UNCLASSIFIED**

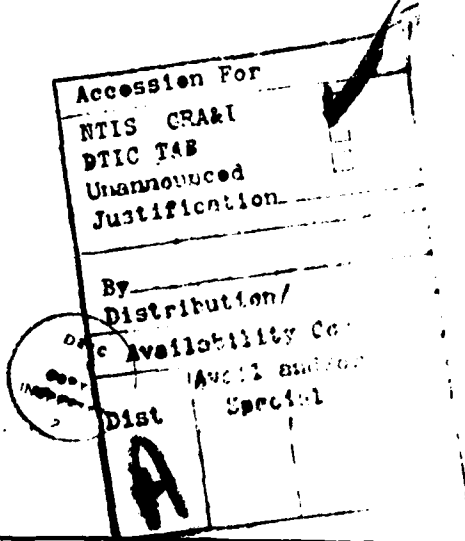
SECURITY CLASSIFICATION OF THIS PAGE(When Data Entered)

object size alone are effective, but the presence of static texture dramatically reduces the effectiveness of changes in object size. In contrast to the traditional emphasis on static picture quality in visual simulation, this finding emphasizes the importance of dynamic parameters in simulation fidelity. In terms of monocular two-dimension simulation of motion in depth, our findings suggest that in many conditions the presence of texture reduces stimulus effectiveness, and at best the presence of texture adds little to the effectiveness of an untextured stimulus.

Subjects cannot accurately locate the center of expansion of an expanding flow pattern in the presence of translational motion of the retinal image when there is no accompanying geometrical distortion. However, subjects are very sensitive to geometrical distortions of the retinal image, and can accurately judge the location of the maximum rate of object magnification even in the presence of translational motion. The relevance of this finding to aviation is that in some (but not all) visual environments the location of the maximum rate of change of magnification due to self-motion approximates the observer's destination.

We have found nerve cells in the visual cortex of cat brain whose properties may in part account for the visual channels for motion in depth.

We have extended our findings on the Williams AFB flight simulator to real telemetry-tracked aircraft at the Yuma TACTS facility. Success in air-to-air combat (A4 versus F-14) and low-level bombing accuracy (A4 aircraft) correlate with laboratory test results on the motion in depth tracking test and expanding flow pattern test, and also correlate with the results of two airborne vision tests.



**UNCLASSIFIED**

SECURITY CLASSIFICATION OF THIS PAGE(When Data Entered)

**AFOSR-TR- 83-0541**

**FINAL TECHNICAL REPORT  
GRANT NO. AFOSR-78-3711**

**ASSESSMENT AND DEVELOPMENT OF OCULOMOTOR FLYING  
SKILLS BY THE APPLICATION OF THE CHANNEL THEORY  
OF VISION**

**DR. D. Regan  
DALHOUSIE UNIVERSITY  
HALIFAX  
NOVA SCOTIA, CN  
B3J 1B6**

**Controlling Office: Air Force Office of Scientific Research/NL  
Bolling AFB, DC 20332**

**Approved for public release;  
distribution unlimited.**

CONTENTS

(a) REPORT DOCUMENTATION

CONTENTS

(b) LIST OF RESEARCH OBJECTIVES

(c) STATUS OF THE RESEARCH EFFORT

Background

Progress October 1, 1981 - September 30, 1982

(d) LIST OF WRITTEN PUBLICATIONS

(e) LIST OF PROFESSIONAL PERSONNEL ASSOCIATED WITH THE RESEARCH EFFORT

(f) INTERACTIONS

f.1 Spoken Papers at Meetings and Conferences

f.2 Consultative and Advisory Functions

(g) NEW DISCOVERIES, INVENTIONS AND PATENT DISCLOSURES STEMMING  
FROM THE RESEARCH EFFORT

AIR FORCE TECHNICAL INFORMATION DIVISION  
NOTICE OF APPROVAL  
THIS IS TO CERTIFY THAT THE INFORMATION CONTAINED  
HEREIN IS APPROVED FOR RELEASE BY THE AIR FORCE  
DISTRIBUTION IS UNRESTRICTED  
MATTHEW J. KELLY  
Chief, Technical Information Division



(b) LIST OF RESEARCH OBJECTIVES

- (1) Define the properties of visual channels that are likely to be involved in aviation.
- (2) Define the visual display features of a flight simulator that contribute to good transfer of training by stimulating the visual channels used in real flying.
- (3) Find how visual channels for form, depth and motion operate when the eyes are moving and when the angle of convergence of the eyes is changing.
- (4) By testing experienced pilots previously rated for visual flying skills in simulators (e.g. for skill in close-formation flying) I aim to identify the channels whose test results predict which pilots will be rated as outstanding (e.g. top 5%) on visual flying skills.
- (5) Having identified the channels whose test results correlate with visual flying skills (Aim #4) I aim to find whether the sensitivities of these channels can be improved by appropriate training procedures (e.g. by simple visual exercises). If so, I aim to find whether these improved test results accurately predict improved visual flying skills as estimated on simulators.
- (6) Design new tests for (a) selecting student pilots, and (b) monitoring the visual abilities of experienced pilots so as to aid in-service retraining programmes for maintaining an adequate level of performance. These tests will measure the sensitivities of the information-processing channels already identified in Aim #1 as likely to be important in practical flying.
- (7) By following student pilots I aim to identify the channels whose test results predict which student pilots who, having passed conventional visual tests, nevertheless will fail to acquire adequate visual flying skills.

(c) STATUS OF THE RESEARCH EFFORT

Background

Visual sensitivity to stereoscopic motion in depth

Tests of stereoscopic depth perception have traditionally been restricted to assessing an individual's ability to see positional (static) depth, and assessing stereoacuity for positional depth<sup>1,2,3</sup>. Similarly, psychophysical research (in man) and single-neuron studies in animals have focussed almost exclusively on positional (static) depth perception<sup>4,5,6</sup>.

In recent years, however, the problem of how we see and judge motion in depth has attracted growing attention. Richards<sup>7</sup> described in 1973 a subject who could hardly see sinewave oscillations in depth if they were of very low frequency, but who could easily see them at 1 Hz. This subject might be described as having lost visual sensitivity to positional (static) depth while retaining sensitivity to motion in depth, so that Richards' observation can be read as evidence for a neural mechanism specifically sensitive to motion in depth.

In 1973 Beverley and I proposed that the human visual system contains channels sensitive to motion in depth that respond only to a restricted range of directions of motion in depth<sup>8</sup>. We argued that there is a separate subsystem for processing motion in depth in addition to the well-known subsystem for processing position in depth. As evidence we cited our findings that: (a) adaptation to motion in depth along some fixed direction in depth depresses visual sensitivity to motion in depth and (b) sensitivity to motion in depth is depressed for only a restricted range of directions of motion in depth. For example, strong adaptation can produce temporary blindness for motion in depth for trajectories directed to the left of the nose, while not affecting visual sensitivity for trajectories directed to the right of the nose.

*First note that, when looking at an object moving in three-dimensional space, the ratio between the velocities of the left retinal image ( $V_L$ ) and the right*



retinal image ( $V_R$ ) directly gives the direction of motion in depth. Figure 1 illustrated this point.

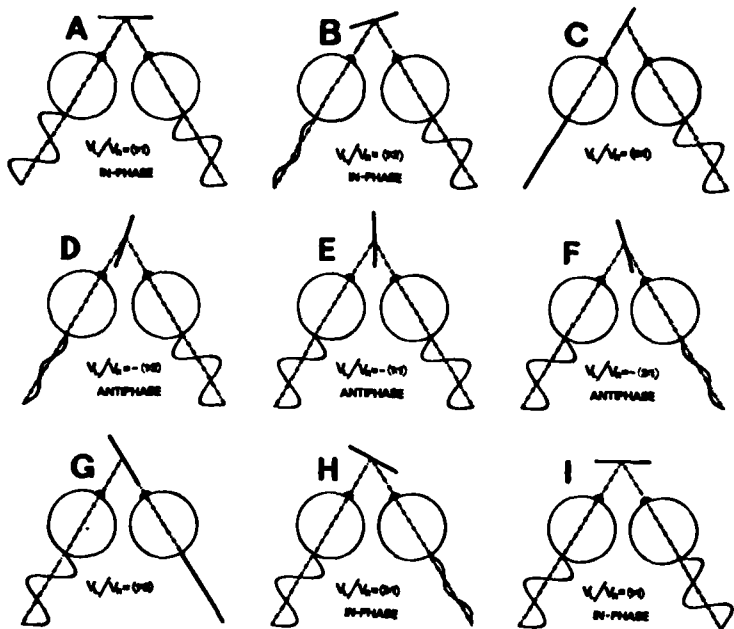
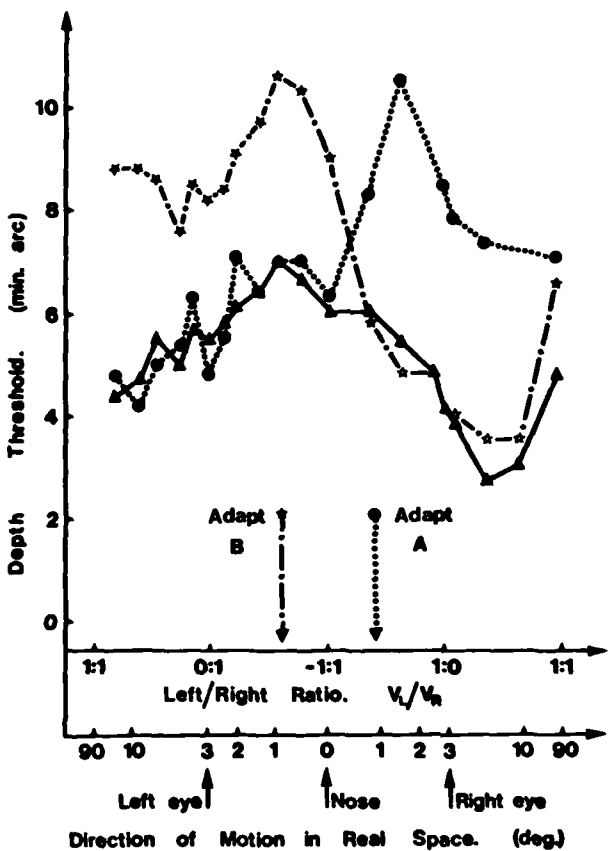


Figure 1. Schematic diagram illustrating the motion of the images on the left and right retinae of a binocularly-viewed stimulus that oscillated in various directions in three-dimensional space. (From Ref. #8)

Figure 2 shows threshold elevations produced by moderate adaptation. The stimulus target oscillated along a straight line in depth at 0.8 cycles/sec with a sinewave motion. Ordinates plot the amplitudes of depth oscillations that could just be seen before and after adaptation. Abscissa plot the ratios ( $V_L/V_R$ ) between the velocities of the left and right retinal images. Abscissae, therefore, plot the directions of motion in depth. For example, with  $V_L/V_R = 1:1$  the target was moving sideways, with  $V_L/V_R = -(0:1)$  the target moved along a line through the left eye, with  $V_L/V_R = -(1:1)$  the target moved along a line through the nose, and with  $V_L/V_R = -(1:0)$  the target moved along a line through the right eye.

Figure 2 shows that there are at least two channels for motion in depth, one sensitive to motion passing to the right of the nose and the other channel sensitive to motion passing to the left of the nose. Further adaptation experiments revealed



**Figure 2.** Directional-specific adaptation to motion in depth. Depth thresholds (ordinates) versus the direction of motion in depth (plotted along the abscissa as  $V_L/V_R$ ). Full line, before adaptation; dotted line, after adaptation to direction A; chain line, after adaptation to direction B. Negative sign means left and right retinal images always moved in opposite directions; positive sign means they moved in the same direction.

that each of these channels was made up of two others. The four directional sensitivity curves are shown in Fig. 3. Note that the inner two curves are so selective that they do not respond at all to trajectories more than  $1.5^\circ$  away from the preferred direction.

Using our method for dissociating the perception of sideways oscillations and motion-in-depth oscillations we showed that, for threshold signals, the bandpass of the motion-in-depth subsystem is centered on a much lower frequency than the bandpass of the subsystem for sideways oscillation<sup>36,37</sup>: the stereoscopic subsystem is very sluggish. These conclusions agree closely with Richard's findings<sup>7</sup> for super-threshold oscillations.

Richards and I provided further evidence for the existence of stereoscopic subsystems for position and for motion. We found that some subjects have regions in the visual field that are blind to motion in depth, but where static depth perception is unimpaired: this implies that two different neural activities or organizations

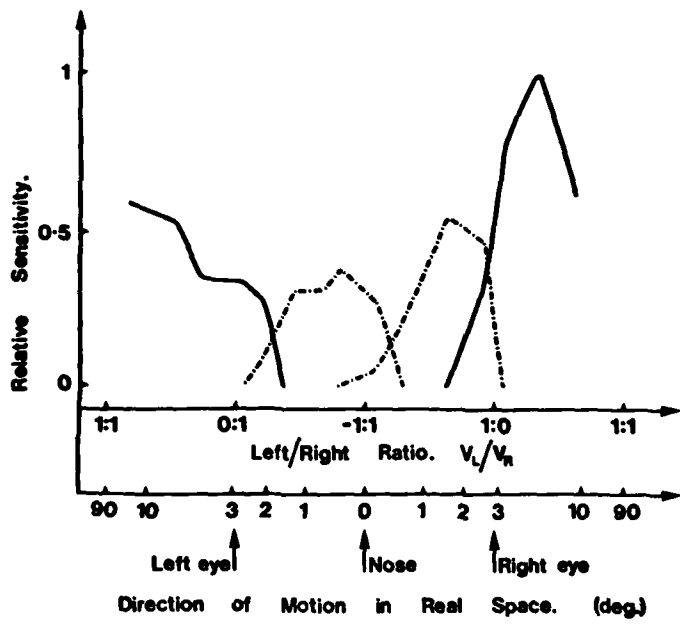


**Figure 3.** Sensitivity curves for four hypothetical channels that underlie the experimentally determined plots of Fig. 2.

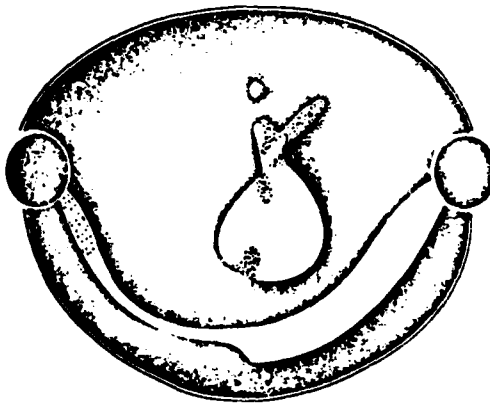
are responsible for processing these two different types of visual information<sup>9</sup>.

Figure 4 illustrates this finding.

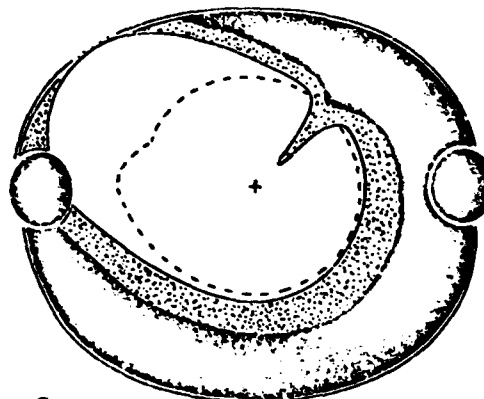
Moving from psychophysical level to single-neuron level Cynader and I<sup>10</sup> have recently found that many neurons in cat visual cortex are preferentially sensitive to motion in depth along a narrow range of directions (Fig. 5). These neurons "throw away" information as to position, while emphasizing information as to the direction of motion in depth (Fig. 6). We emphasized that previous neurophysiologists had not found these neurons because they did not look for them (by using appropriate stimulation): previous workers looked only for position-in-depth neurons. Our motion-in-depth cells do not reveal their properties unless they are appropriately stimulated.



**A** Stereo field plot for a convergent stimulus disparity, obtained using a  $1^\circ$  bar oscillating back and forth from 0 to  $0.4^\circ$  disparity twice per second. The two ovals on the horizontal axis are the blind spots. The dark regions inside the double-line perimeter indicate regions of no depth. (The field was not explored beyond the perimeter shown.) The dotted areas are regions of amblyopia, where unstable depth sensations could occasionally be elicited. The cross corresponds to the central fovea. Subject DR.



**B** DIVERGENT  
Stereo field plot for a divergent stimulus disparity for subject DR. Except for reversing the bars presented to each eye (a sign reversal), the stimulus is identical to that used to obtain the field shown in **A**.



**C** Solid curve encompasses the region of the visual field over which DR can see a  $0.4^\circ$  divergent stimulus disparity presented as a 100 msec. flash. Dashed curve is same stimulus as used to construct **B** except that the oscillating bar is flickered on and off 1.5 times per second.

Figure 4. From Reference #9.

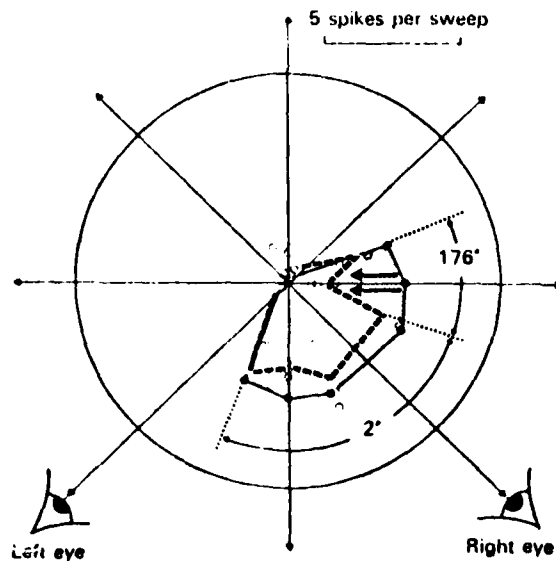


Note that the motion-in-depth channels (or neurons) signal "I don't know where it is or what it is, but it is going to hit (or miss) you". They signal this with much more precision, and for objects at much greater distances than could be done by the classical positional-depth stereoscopic subsystem. We pointed out<sup>8,10</sup> that this subsystem may also be used when subjects move relative to the outside world, e.g. when landing an airplane or flying in close formation and in driving an automobile.

Turning back to studies of human performance, Beverley and I measured human visual ability to discriminate between two direction of motion in depth<sup>11</sup>. We found that our measured discrimination was in line with our estimations of certain acute oculmotor skills of baseball and cricket players ( $0.2^{\circ}$  precision in discriminating the direction of motion in depth). These data, shown in Fig. 7, might be read as an indication of the limiting precision with which a pilot could be expected to visually judge his direction of flight if he were restricted to stereoscopic motion cues alone.

However, even the sharp selectivity of our proposed stereoscopic motion mechanisms (e.g. sensitive to only a  $1.5^{\circ}$  range of directions, Fig. 3) cannot explain discrimination so exquisite as  $0.2^{\circ}$ . We were therefore forced to propose an additional mechanism. Our discrimination data suggested to us that human ability to make very acute distinctions between directions of motion in depth is based on subtraction mechanisms (much as, in colour vision, the very acute human sensitivity to differences in wavelength is based on opponent-colour subtraction processes). Figure 8 is a psychophysical model that outlines our ideas. Note that the binocular motion filters OR, IR, IC and OL in Fig. 8 have now been associated with classes of single neuron in parastriate cortex<sup>10,13</sup>.

This line of research is summarized in Reference #12 and Reference #13.

Figure 5. From Reference #10.

**Fig. 5** Binocular selectivity for the direction of motion plotted in polar co-ordinates looking down onto the left and right eyes. Same unit as in Fig. 3. The number of spikes per sweep for 20 stimulus cycles at 37 deg/sec is plotted radially on a linear scale (dashed line, open circles). The fine continuous line (filled circles) shows the linear sum of responses to separate stimulations of the left and right eyes: each point is based on separate empirical measurements. This Figure shows how the inhibition for binocularly viewed sideways motion (arrowed) had the effect that appreciable responses were generated by only a narrow ( $2^\circ$ ) range of directions of motion for which the target would either hit or narrowly miss the animal's head.

The number of spikes per sweep for 20 stimulus cycles is plotted radially on a linear scale. The ratio between the speeds of the left and right retinal image is plotted linearly round the circumference of the circle. For explanatory purposes, the corresponding angular directions in real space are also shown, in this case for a viewing distance of 145 cm and interpupillary separation of 3.0 cm. Note that this angular scale is very nonlinear, and emphasizes the  $2-4^\circ$  range of directions that pass between the eyes at the expense of the remaining  $357-6^\circ$  range of directions that miss the head.

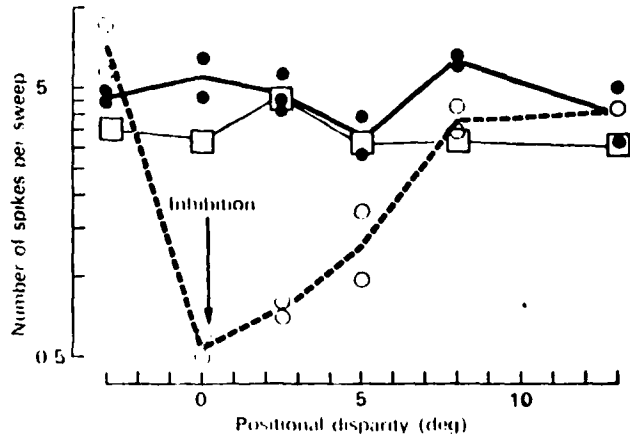


**Fig. 6** A unit that was preferentially sensitive to motion directed between the eyes. The number of spikes per sweep in 20 stimulus cycles at 37 deg/sec is plotted logarithmically as ordinates versus the positional disparity between the left and right bars (plotted linearly). In this, as in all subsequent Figures, the zero of disparity is arbitrary. The fine continuous line plots the linear sum of response to separate stimulations of the left and the right eyes. The heavy dashed line shows that responses were inhibited tenfold below this linear prediction when the left and right eyes were simultaneously stimulated with identical movements (i.e. binocularly viewed sideways motion, cf. Fig. 1). The arrow indicates the depth of this inhibition which clearly extended over a broad range of disparities. The full line shows that no such inhibition occurred when left and right eyes were stimulated with identical speeds in opposite directions (i.e. binocularly viewed motion directed along a line midway between the eyes, cf. Fig. 1). Thus, over a large volume of space, an inhibitory mechanism caused this unit to favour motion directed between eyes over sideways motion. The preferred orientation was  $15^\circ$  clockwise from vertical.

Figure 7. From Reference #11.

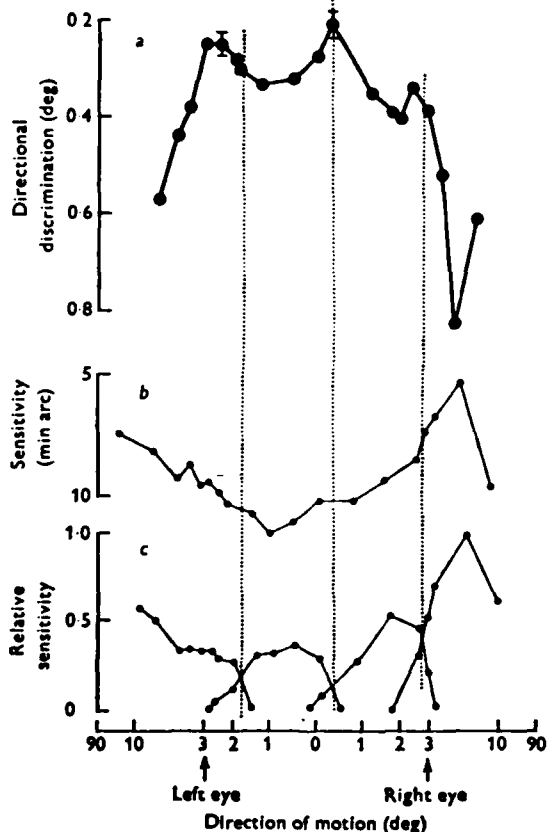


Fig. 7 a, discrimination of the direction of movement in depth. Discrimination is plotted as ordinates, the directions of the target's trajectories as abscissae. Standard deviations are shown for one measurement of 200 judgements; each point is based on between two and six such measurements.

b, sensitivity to movement in depth. The peak-peak oscillations of disparity that can just be seen are plotted as ordinates (in min arc) and the directions of the targets' trajectories as abscissae.

c, sensitivity curves of four hypothetical groups of binocular mechanisms tuned to different directions of movement in depth.

Figure 8. From Reference #11.

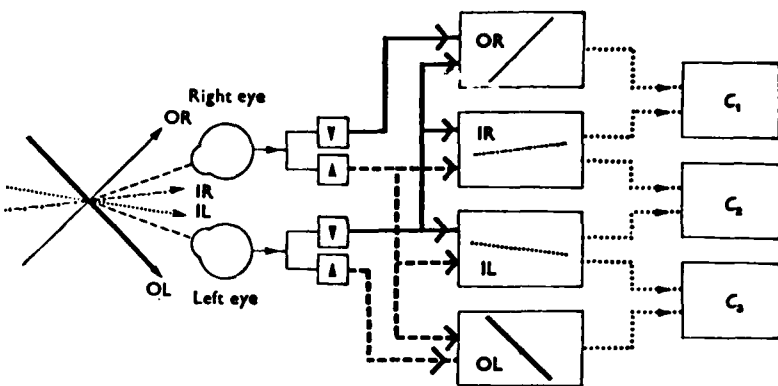


Fig. 8. Each eye drives one pool of motion detectors sensitive to left-right horizontal motion and another pool sensitive to right-left motion. The outputs of these four pools of monocular motion detectors are routed in such a way that there are four pools of binocular movement detectors sensitive to movements along four different directions in three dimensions. Thus, the directionally tuned motion detector OR is most sensitive to movement along the direction OR, the detector IR is tuned to the direction IR, and so on. The outputs of these four pools of binocular detectors are compared at comparators  $C_1$ ,  $C_2$  and  $C_3$  so as to enhance the discrimination of direction. The comparison process incidentally produces characteristic maxima in the discrimination curve of Fig. 7 a.

Note that this Figure covers motion directed only towards the subject. For movements away from the subject there is an additional set of four boxes OR, IR, IL and OL. For movement in either direction the boxes OR and IR respond only when the left eye's image moves faster than the right eye's, while IL and OL respond only when the right eye's image moves faster than the left eye's.



Note that the human stereoscopic sensitivity to motion in depth that we have measured is not predictable from conventional measurements of positional (static) depth sensitivity.

Changing size as a cue to motion in depth

It is well known that changing size is a cue to motion in depth. We have recently shown that, in man, information as to changing size is processed in separate channels<sup>14</sup>. These channels are quite distinct from the channels for sideways motion (Fig. 9). The sensitivity, dynamics and fatiguability of the changing-size channel differs between individuals, and does not seem to be predictable from other visual measurements. On the basis of our psychophysical data we have suggested that the changing-size channel corresponds to a previously-unknown and very specific neural mechanism in the visual pathway<sup>14,15,16,17</sup>. Our recent single-neuron evidence is that such a physical mechanism does indeed exist in cat visual cortex<sup>18</sup>.

Visual acuity and visual sensitivity to spatial frequency

There is good psychophysical evidence that an image of the outside world formed on the retina is split up into components of different spatial frequencies by a process resembling spatial Fourier analysis<sup>19,20,21</sup>. This analysis is carried out by parallel information-processing channels, each sensitive to a narrow range of spatial frequencies of a particular orientation. Although this "spatial frequency channel" hypothesis is certainly not the only fruitful basis for research on form vision<sup>22,23</sup>, it has been most influential in drawing attention to the need for a fresh approach to practical tests of visual acuity. Since conventional measures of visual acuity (e.g., Snellen) test only the ability to see very fine, high-contrast detail, such conventional procedures examine only the channels sensitive to high spatial frequencies and entirely miss channels sensitive to medium and low spatial

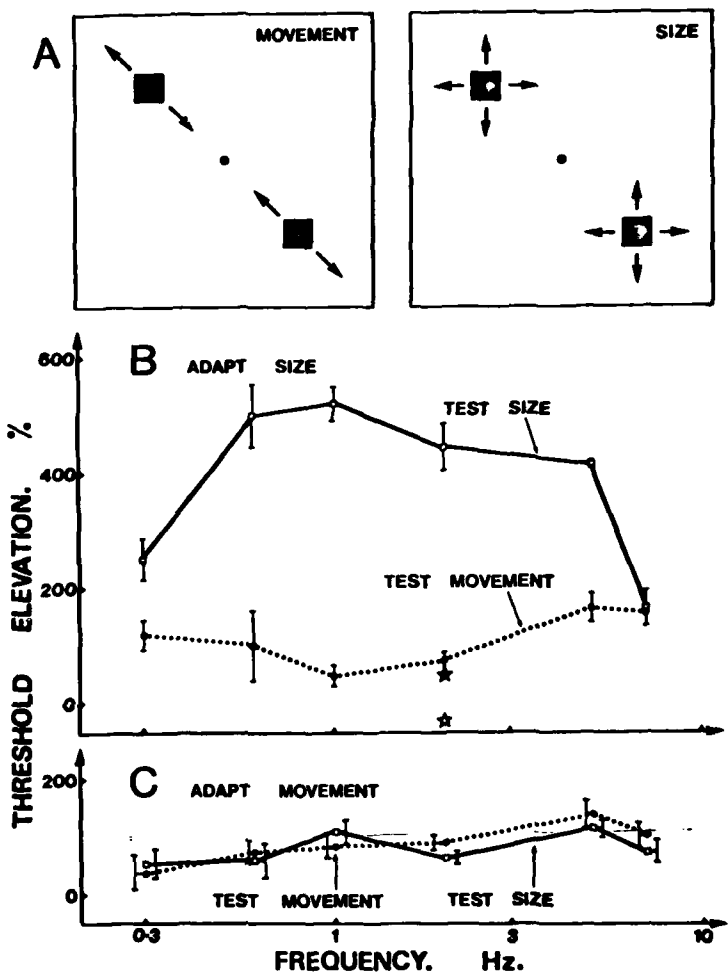


*Figure 9.* Adapting to oscillating size preferentially depressed visual sensitivity to oscillating size. The stimulus was two identical squares on either side of a fixation spot (A). Ordinates plot percentage elevations of visual threshold produced by 25 mins adaptation to 2 Hz oscillating size (B) and 2 Hz oscillatory motion (C). Test frequencies are plotted as abscissae. Vertical lines show  $\pm 1$  SE. The large filled star and large open star show threshold elevations produced by adapting to 2 Hz flicker upon sensitivity to oscillating size and oscillatory motion, respectively. From Reference #14.

frequencies.

That this deficiency in conventional testing can be serious in practice is illustrated by our own recent findings<sup>24</sup> and by those of Capt. Ginsburg (Wright-



Patterson AFB). We find that a considerable proportion of multiple sclerosis patients have visual defects that are not revealed by the Snellen test, but are evident to the spatial-frequency grating test (28/48 patients). In particular, 14/48 patients experienced degraded sensitivity to coarse and medium-coarse detail (i.e., low and medium spatial frequencies) although sensitivity for fine detail was unaffected so that the Snellen acuity was normal (20/20). Figure 10 illustrates a sensitivity loss restricted to medium spatial frequencies.

More to the point, our data for normal control subjects showed a considerable range of sensitivities to coarse and medium-coarse detail, a variability that was not detected by the Snellen test. In other words, visual defects of patients such as those shown in Fig. 10 were only different in degree from variations within the normal control group. Therefore, if visual acuity screening for aircrew were restricted to the Snellen type of test, then some pilots would necessarily have poor low-contrast vision at medium and low spatial frequencies, and there would be no indication of this except possibly in flying performance under hazy or low-contrast conditions.

#### Interactions between different visual cues

In assessing visual function it is usual to test each visual parameter separately. It might seem reasonable to assume that a visual stimulus providing two cues should be easier to see than a stimulus providing only one cue, all other things being equal. But this is not necessarily true in practice. For example, a moving object may move in depth (providing two cues, namely retinal image movement) or may move in depth (providing two cues, namely retinal image movement and changing disparity). Beverley and I found that the two cues might add or might cancel, so that depth movement could be either easier to see or more difficult to see than sideways movement, depending on the stimulus situation<sup>25,26</sup>.

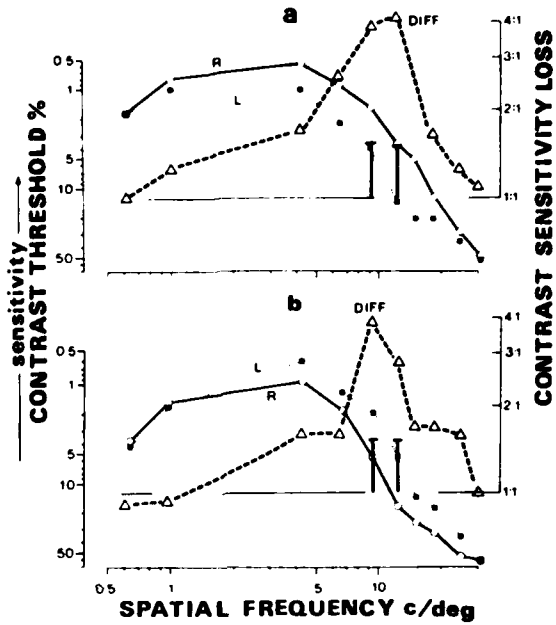


*Figure 10* Illustrates how multiple sclerosis can selectively degrade visual sensitivity for medium spatial frequencies. Visual sensitivity to a grating (ordinates, left side) plotted versus the grating's spatial frequency (abscissae in cycles per degree). Continuous line for right eye, dotted line for left. Dashed line plots difference between visual sensitivities for left and right eyes expressed as a ratio. Note that the two eyes have similar sensitivities at high and low spatial frequencies. Results shown for two patients. Note that sensitivity increases upwards.

*From Reference #24.*

In the real visual world it is common for several cues to be present simultaneously, so that visual tests should also look for interactions between cues if they are to be effective predictors of real-world eye-limb coordination.



### Flow patterns and changing-size channels

Figure 11 is the well-known illustration from J. J. Gibson's 1947 Air Force Report.<sup>27</sup> The superposed arrows indicate that, as the pilot moves towards a point on the ground, the visual scene appears to flow radially from that point. The arrows indicate that the rate of flow increases with distance from the point of impact.

During the Second World War J. J. Gibson investigated the use of movie displays as an aid to flying training. In his 1947 report he showed that the visual flow pattern is an important cue to the direction of motion, and is used by pilots as a basis for visual judgements during landing.<sup>27</sup>

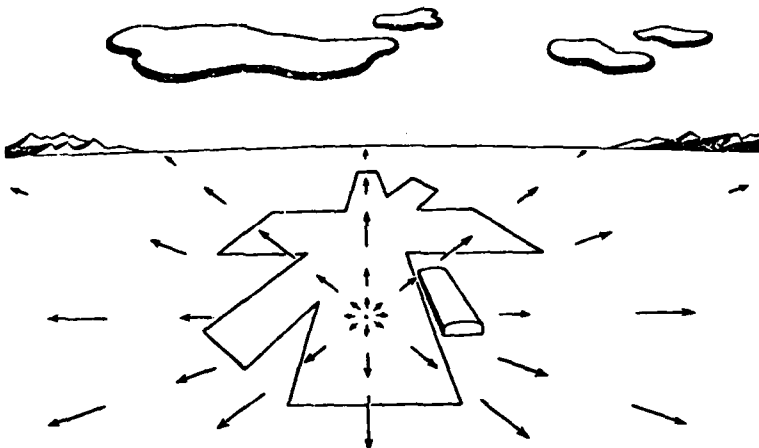


FIGURE 11 Gradients of Deformation during a Landing Glide



Gibson's finding could be taken as a hint that the human visual system might contain a neural organisation that is sensitive to flow patterns, but is relatively insensitive both to local motion and to the local changes of luminance that accompany flow patterns since these can occur in the absence of flow patterns. One way of attaining preferential sensitivity to flow patterns would be by responding only to certain relationships between local motion in different regions of the visual field. At first sight this seems to demand interactions across considerable distances in the visual field.

What we have recently shown is that visual sensitivity to flow patterns can be explained in simple terms, without involving such long-range interactions.<sup>28</sup>

We proposed that a flow pattern could stimulate our changing-size channel, and furthermore that the relative activities of changing-size channels fed from adjacent regions of the visual field could provide a basis for locating the focus of a flow pattern. This proposal is illustrated in Figure 12. For simplicity the receptive field of a changing-size channel is shown in Figures 12B, C, D as a square. We suppose that the flow pattern would stimulate a changing-size channel sensitive to expansion (size increase) when the focus F fell within the receptive field as in Figures 12B or 12C. On the other hand, the changing-size filter would be stimulated more weakly (or not at all) when the focus F lay outside its receptive field (as in Figure 12D). Therefore, a neural mechanism that compared the outputs of changing-size filters fed from nearby regions of the visual field would provide a basis for estimating the position of the focus F rather precisely. The smaller the dimensions of the changing-size receptive field, the more precisely could the position of the focus F be estimated.

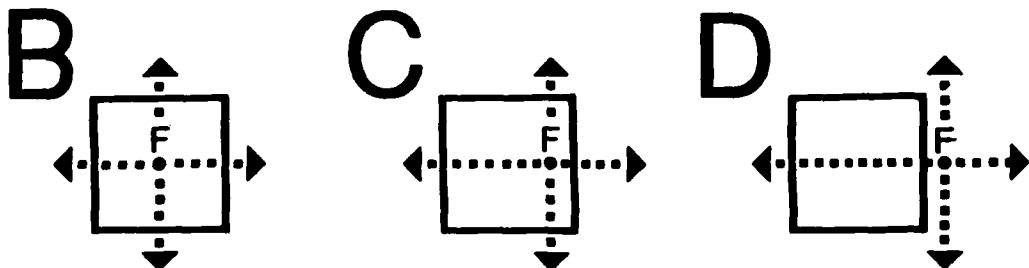


**Figure 12 B, C, D** The human visual system contains channels sensitive to changing-size. A changing-size channel will respond to the flow pattern when the flow pattern's focus  $F$  falls inside the channel's receptive field (represented by the square) but not when  $F$  lies outside the receptive field. Figure 13 presents evidence that this could provide a basis for judging the position of a flow pattern's focus. Such judgements would be precise, since the receptive field of a changing-size channel is no more than  $1.0^\circ$  to  $1.5^\circ$  in diameter.<sup>16</sup>

We tested this idea experimentally by finding whether gazing at a flow pattern for some time preferentially reduced visual sensitivity to changing-size, and if so whether this effect was greater in the immediate neighbourhood of the flow pattern's focus than in the regions remote from the focus.\* We measured visual sensitivity to changing-size by stimulating the eye with a test rectangle whose horizontal edges were stationary but whose vertical edges oscillated from side-to-side at 1 Hz in antiphase (i.e. moved in opposite directions at any given instant; Figure 13A). Control experiments differed in only one respect, namely that the test rectangle's vertical edges oscillated inphase rather than in antiphase (i.e. in control experiments

\* We used the electronically-generated flow pattern illustrated in Figure 13B as an equivalent of a realworld flow pattern. In our simplified flow pattern, however, the radial velocity of flow was constant over the screen. A simple calculation shows that in a realworld flow pattern the angular velocity of flow for an object point located along a direction  $\theta^\circ$  from the point towards which the eye is moving is proportional to  $\theta V/D$  where  $D$  is the distance between the eye and the object point and  $V$  is the linear velocity of locomotion.

We plan to move closer to the realworld situation in later experiments (see below).



the edges moved in the same direction at any given instant, so that the rectangle's size remained constant, but its position oscillated). Subjects adjusted the amplitude of the oscillation so that it was just visible. We recorded these threshold settings before and after 10-min inspection of the flow pattern illustrated in Figure 13B. By calculating the percentage changes of threshold we obtained a measure of the changes in visual sensitivities to the antiphase and inphase test rectangles caused by inspecting the flow pattern.

Threshold elevations for the antiphase (changing-size) test rectangle were plotted as ordinates in Figure 13C versus the distance  $X^\circ$  between the centre of the test rectangle and the focus of the adapting flow pattern. Inspecting the flow pattern produced clear depressions of visual sensitivity to the antiphase test rectangle. But this adapting effect fell to insignificant levels when the centre of the  $0.5^\circ$ -wide test rectangle was located only a little more than  $0.25^\circ$  from the point in the visual field previously occupied by the focus of the adapting flow pattern. Our findings are consistent with the prediction illustrated in Figure 12B, C and D that threshold elevations should fall to zero when the focus of the flow pattern was located outside the receptive field of the changing-size channel (neglecting the effect of fixation variations due to eye movements), and suggest that the receptive field of the channel we were testing had approximately the same width as the  $0.5^\circ$  test stimulus rectangle.

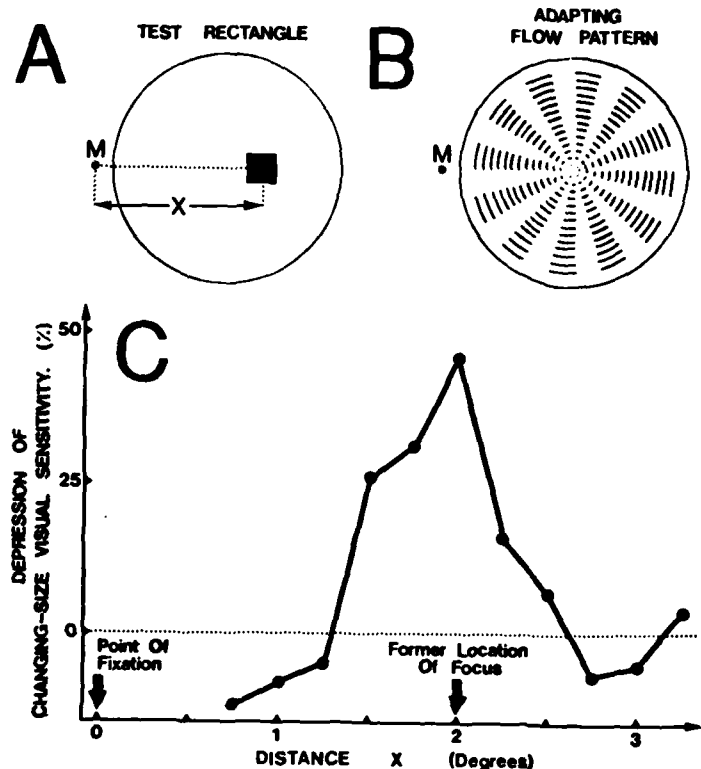


Figure 13

**A** The vertical edges of the test rectangle oscillated from side-to-side in antiphase (i.e. test changing-size) on inphase. Oscillation thresholds were measured as a function of  $X^\circ$  before and after 10 min inspection of the flow pattern. The edges were moved by a triangular waveform, i.e. at constant speed. Three test rectangles were used in separate experiments. Their widths were  $0.25^\circ$ ,  $0.5^\circ$  and  $1.0^\circ$ . All were  $0.5^\circ$  high. Total light flux was constant.

**B** Flow pattern of  $3.5^\circ$  diameter consisting of 48 equally-spaced sectors, alternate sectors containing 13 line segments. The line segments flowed radially outwards from the focus for 5 sec, then reversed their directions of motion for 5 sec, and so on. The flow pattern and the test rectangle were never visible at the same time. Subjects were allowed 10 sec

inspection of the test rectangle to make a setting. Sixty sec exposure to the adapting flow pattern intervened between successive postadaptation settings while 60 sec exposure to the stationary flow pattern intervened between successive preadaptation settings. A green LED of luminance  $13 \text{ cd m}^{-2}$  served as fixation mark (M). The right eye only was used. The radial velocity of flow was  $0.75 \text{ deg sec}^{-1}$ , and was constant across the screen.

**C** Threshold elevations for the  $0.5^\circ$  antiphase test rectangle (ordinates) versus distance  $X^\circ$ .

Our control data showed that threshold elevations for inphase oscillations of the test rectangle's edges were much smaller than the threshold elevations for anti-phase oscillations shown in Figure 13C. Furthermore, the inphase elevations did not depend upon the distance  $X^\circ$  from the focus.

Our previous finding that changing-size channels are not sensitive to pairs of edges more than about  $1.5^\circ$  apart<sup>16</sup> make sense in the light of our present proposal that



a major function of changing-size channels might be to provide a basis for judging the location of a flow pattern's focus, since changing-size channels sensitive to narrow objects would signal the location of the focus more precisely than changing-size channels sensitive to wide objects.

Our chief conclusion is that visual sensitivity to the location of a flow pattern's focus could be mediated by channels that respond to changes in the size of small objects. The relative activities of these changing-size channels might be one basis on which the brain computes the direction in which the head moves with respect to the external world.

*If visual sensitivity to flow patterns is important in landing aircraft and in automobile driving, and if this visual capacity proves to be relatively uncorrelated with the results of standard visual tests, then there may be flying and driving tasks for which tests of sensitivity to flow patterns or to changing-size might profitably be added to the present battery of screening tests.*

#### Binocular and monocular stimuli for motion in depth

The results reported in this section bear on the question "what effect would a sudden loss of binocular vision have on visual judgements of motion in depth". The results reported here are, therefore, relevant to how a loss of binocular vision might affect landing performance.<sup>29</sup>

Figure 14 deals with the point that a sensation of motion in depth can be produced in two quite different ways, namely by stimulating the eye with changing-size ( $\dot{\theta}_S$  min arc sec<sup>-1</sup>) or with changing-disparity ( $\dot{\theta}_D$  min arc sec<sup>-1</sup>). Changing-size stimulation can be either monocular or binocular, but changing-disparity can only be binocular. The heavy continuous line and the heavy dashed line plot the amplitudes of changing-size stimulation and changing-disparity stimulation that

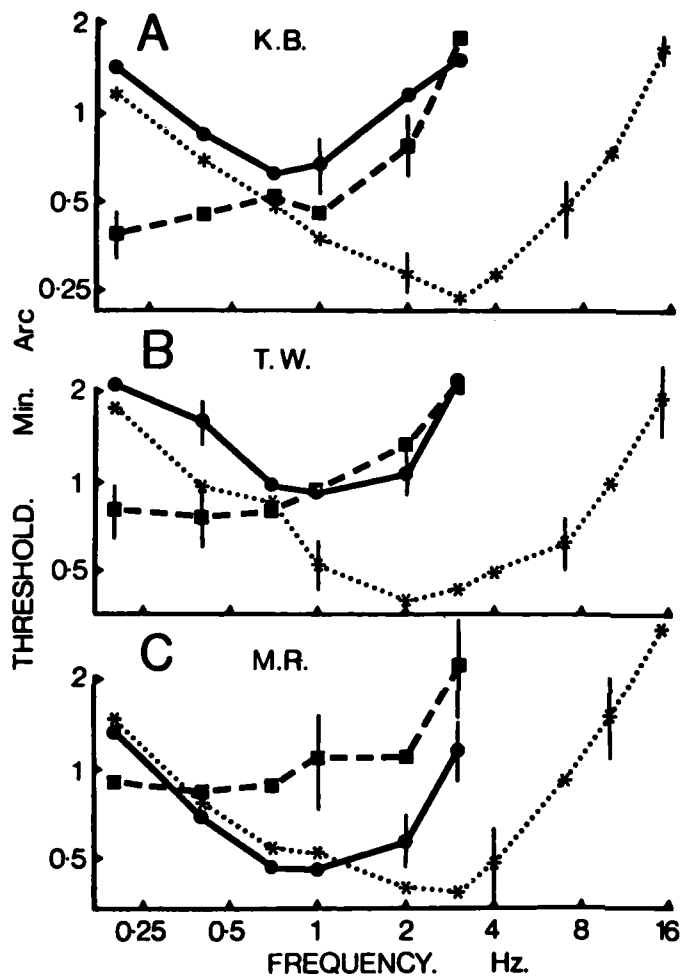


**Figure 14** Modulation transfer functions for changing-size sensation and motion-in-depth sensation.

in terms of the psychophysical model that we proposed to explain other data.

Now we turn to the relative effectiveness of changing-size and changing-disparity stimulation as stimuli for motion in depth sensation. Figures 17 and 18 show that the relative effectiveness is not constant, but depends on speed (Figure 17) and on inspection time (Figure 18).

just produce a sensation of motion in depth. Visual sensitivities are clearly different at low repetition frequencies.

Note also that a single stimulus (namely, changing size) can produce two quite different sensations, namely changing-size and movement in depth. The fine dotted line plots amplitudes of changing-size stimulation that produced a just-detectable sensation of changing-size. Comparing the fine dotted line with the heavy continuous line, it is clear that there is a large difference between sensitivity for the two sensations from about 1 Hz upwards.

These different modulation transfer functions can be understood

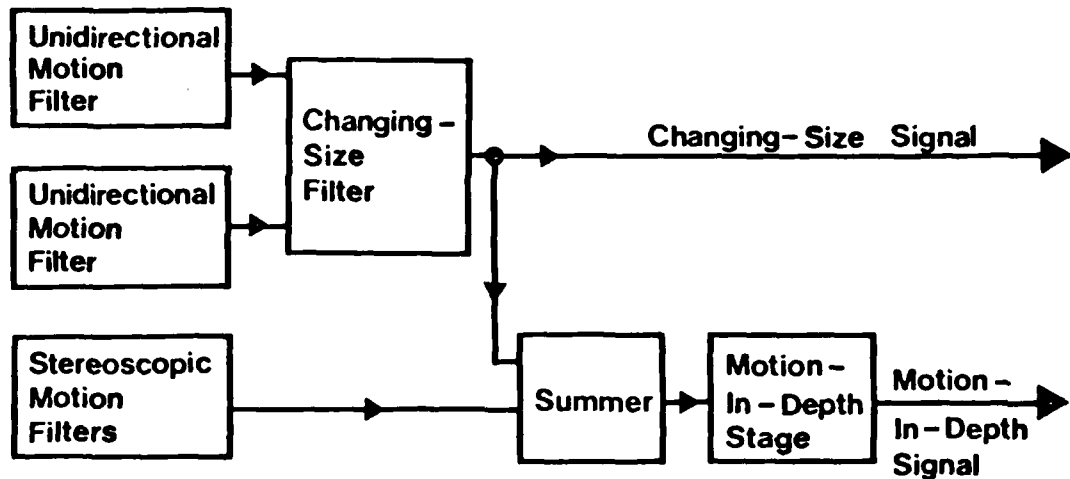


Figure 15 *Psychophysical model* STEREOSCOPIC MOTION FILTERS compute the relative velocities of the left and right retinal images, and are thus selectively sensitive to the direction of motion in depth. When the opposite edges of a target move in opposite directions UNIDIRECTIONAL MOTION FILTERS drive a CHANGING SIZE FILTER that produces a changing-size signal and also drives a MOTION IN DEPTH STAGE that outputs a motion-in-depth signal. The stereoscopic motion filter also drives the motion-in-depth stage.

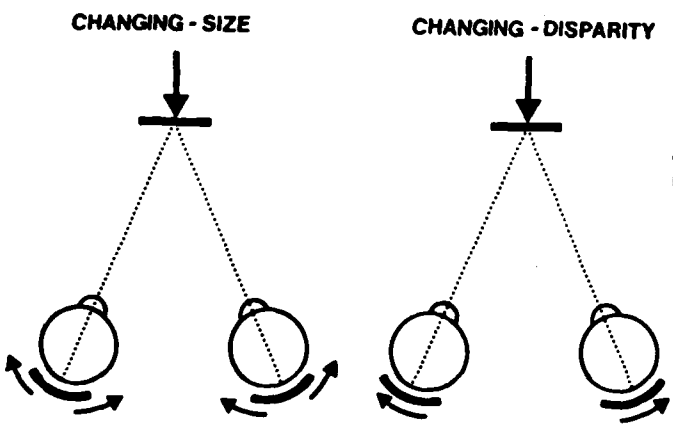


Figure 16 This figure illustrates the changing-size and changing-disparity stimulation in the left and right eyes that is produced by a realworld object moving towards the head. In our experiments of Figures 17 and 18 we opposed changing-size and changing-disparity stimulation. In these experiments, changing-disparity was as illustrated in Figure 16, but the size was decreasing instead of increasing.<sup>29</sup>

We generated a stimulus that never occurs in the everyday visual world. The stimulus rectangle's disparity increased so as to indicate that the square was coming closer, but its size decreased, indicating that it was going away (Figure 16).

We found that by opposing  $\dot{\theta}_S$  and  $\dot{\theta}_D$  in this way we could cancel the sensation of motion in depth, and thus measure relative visual sensitivity to  $\dot{\theta}_S$  and  $\dot{\theta}_D$ . The ratio  $\dot{\theta}_D/\dot{\theta}_S$  for which motion-in-depth was just cancelled we took as a measure of relative sensitivity.

Figure 17 shows that the relative effectiveness of  $\dot{\theta}_D$  and  $\dot{\theta}_S$  as stimuli for motion in depth depended on speed (i.e. on  $\dot{\theta}_S$ ). The relative effectiveness of changing-disparity progressively increased as speed was increased.

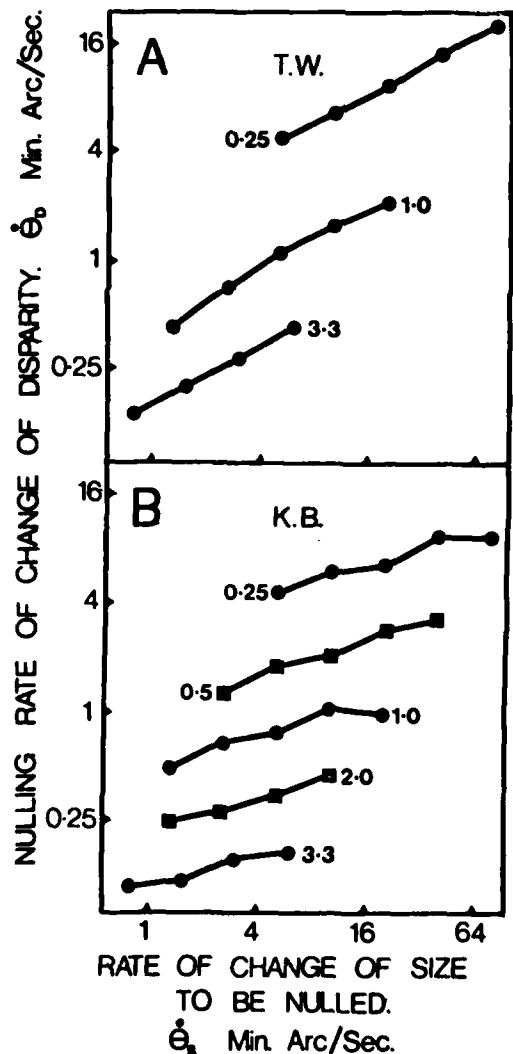


Figure 17 Cancellation of motion-in-depth sensation by opposing changing-size and changing-disparity stimuli: effect of velocity. The subject viewed a square, each of whose edges moved outwards at constant speed for either 0.25 sec, 1.0 sec or 3.3 sec as marked on the figure. The square then disappeared for 0.25 sec and the cycle repeated. Abscissae plot  $\dot{\theta}_S$  where  $\dot{\theta}_S/2$  is the rate of change of side length in min arc sec<sup>-1</sup>). Ordinates plot the rate of change of binocular disparity ( $\dot{\theta}_D$  min arc sec<sup>-1</sup>) required to cancel the sensation of motion in depth produced by the rate of change of size  $\dot{\theta}_S$ . A - subject T.W. B - subject K.B. From Reference #29.

In Figure 18 we varied the stimulus inspection time from 0.25 sec to 4.0 sec. Figure 17 shows that the relative effectiveness of  $\dot{\theta}_D$  and  $\dot{\theta}_S$  as stimuli for motion in depth depended on the inspection time. Changing-disparity grew progressively less effective as inspection time was reduced.

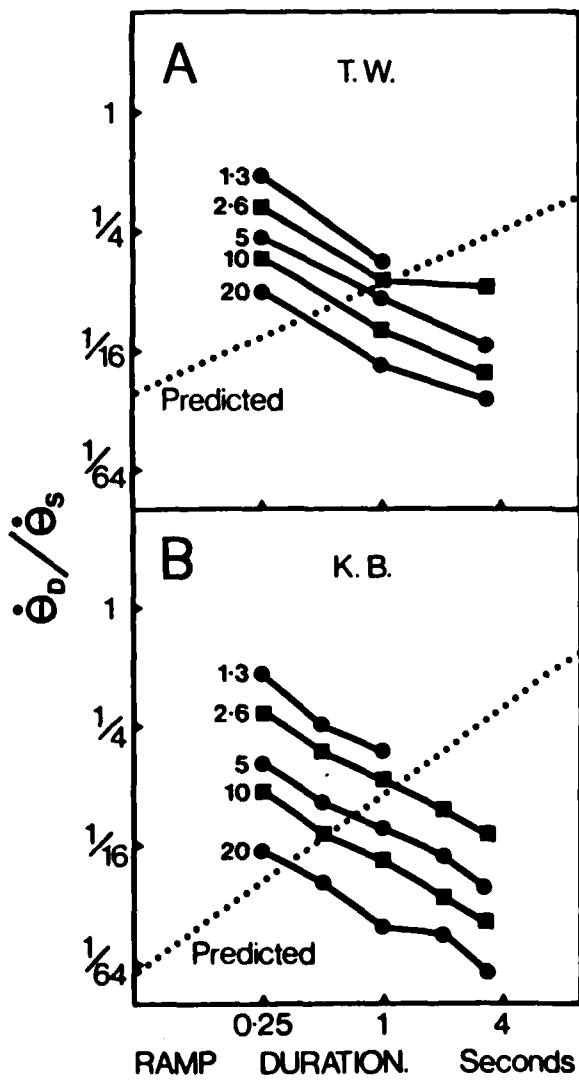


Figure 18 Relative effectiveness of changing-disparity and changing-size as stimuli for motion-in-depth: effect of inspection time.

A  $1^\circ \times 1^\circ$  square changed size at a fixed rate ( $\dot{\theta}_S/2 \text{ min arc sec}^{-1}$ ) for a ramp duration  $t$  secs, then disappeared for 0.25 sec and the cycle repeated. Ordinates plot  $\dot{\theta}_D/\dot{\theta}_S$  where  $\dot{\theta}_D$  is the rate of change of disparity required to cancel the sensation of motion in depth produced by a given rate of change of size ( $\dot{\theta}_S$ ). Abscissae plot ramp durations. The numbers by the plots indicate the amplitudes of the size change during the ramp.

A - subject T.W. B - subject K.B.  
 From Reference # 29.

The data shown in Figures 17 and 18 suggest that the question "what effect would a sudden loss of binocular vision have on landing performance" does not have a single, generally-valid answer. A sudden loss of binocular vision would remove the stimulus of changing-disparity, while leaving changing-size as a stimulus for motion in depth. If we are correct in our suggestion that changing-size channels mediate visual judgements of flow patterns, then a loss of binocular vision would not have a great effect on this visual function (we find that sensitivity would drop by about 1.2-1.4 times). On the other hand, visual sensitivity to motion in depth might or might not be strongly affected. The following factors would be involved:

(1) Inspection duration. Motion-in-depth sensitivity for short inspection durations would be less affected by losing binocular vision.

(2) The target's velocity in depth. Motion-in-depth sensitivity at low velocities would be less affected by losing binocular vision.

(3) The absolute width of the object. Motion-in-depth sensitivity for wide objects would be less affected by losing binocular vision.

(4) The difference between binocular and monocular thresholds for motion-in-depth sensation produced by changing-size stimulation.

(5) Intersubject differences. These are large. Even over our small sample of five subjects we found 80:1 intersubject differences in the relative effectiveness of changing-size and changing-disparity as stimuli for motion in depth.

Summarising, we would expect that after a sudden loss of binocular vision it would be more difficult to see a weak flow pattern (sensitivity down by 1.2-1.4), but once seen, the ability to locate the focus would be little degraded. Therefore, the only effect would be that the pilot would not be able to use the flow pattern until he was closer to the landing field. However, when he was close to the ground

the result of losing binocular vision might be more serious since the pilot might then require to judge the speed of motion in depth. A sudden loss of binocular vision (i.e. the removal of  $\dot{\theta}_D$  stimulation) could degrade movement-in-depth judgements especially for small objects and high speeds, but this would depend very much on the individual (see above).

The relative effectiveness of changing-size ( $\dot{\theta}_S$ ) and changing-disparity ( $\dot{\theta}_D$ ) as stimuli for motion-in-depth does not depend on viewing distance

It is well known that stereoscopic depth perception is very insensitive at distances greater than about 10 metres. In view of this it may seem surprising that relative sensitivity to changing-disparity ( $\dot{\theta}_D$ ) and to changing-size ( $\dot{\theta}_S$ ) does not depend on viewing distance. A simplified version of our proof is given in Figure 19.

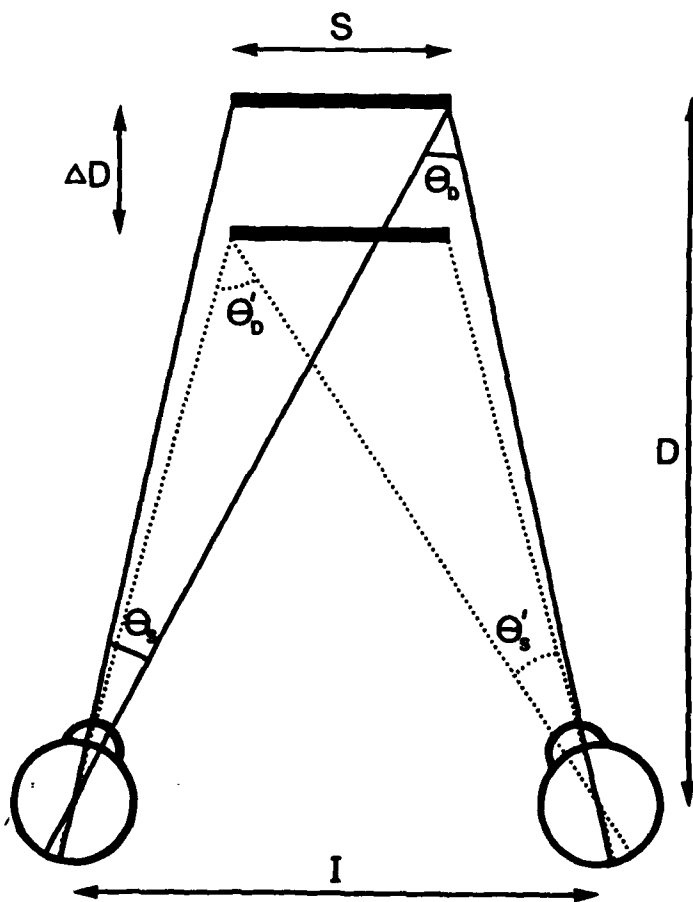


Figure 19 A stimulus correlate of an object's absolute linear width.

$$\text{Approximately } \dot{\theta}_D = \frac{I}{D}, \quad \dot{\theta}'_D = \frac{I}{(D-\Delta D)},$$

$$\dot{\theta}_S = \frac{S}{D} \text{ and } \dot{\theta}'_S = \frac{S}{(D-\Delta D)}. \text{ Hence} \\ (\dot{\theta}'_D - \dot{\theta}_D) = \Delta \dot{\theta}_D = \frac{I \Delta D}{D^2} \text{ and } (\dot{\theta}'_S - \dot{\theta}_S) = \\ \Delta \dot{\theta}_S = \frac{S \Delta D}{D^2}. \text{ Thus } \frac{\Delta \dot{\theta}_S}{\Delta \dot{\theta}_D} = \frac{S}{I}. \text{ Hence} \\ \dot{\theta}_S / \dot{\theta}_D = \frac{S}{I}. \text{ In words: width of object}$$

$(S) = I \times (\text{Rate of change of angular width} : \text{Rate of change of angular disparity})$ . Note that this gives the object's width independently of its distance, and that the visual system contains channels for  $\dot{\theta}_S$  and  $\dot{\theta}_D$  so that the absolute value of  $S$  is, in principle, available to the visual system. From Reference #29.

Practical calculations of the relative effectiveness of binocular and monocular cues for motion-in-depth

The experimental measurements of Figure 18 and the theory of Figure 19 allow us to calculate the relative effectiveness of binocular and monocular cues to motion in depth in practical cases. For example, we can predict the effect of closing one eye upon motion-in-depth perception when travelling at a given velocity at a given distance from the landing point.

In order to illustrate the extent to which the relative effectiveness of changing-disparity and changing-size as stimuli for motion-in-depth depends on the stimulus situation I have calculated three real-world examples, choosing extreme visual conditions. (These calculations are by way of illustration only.) The method of calculation is set out below in single spacing, and the values of  $\dot{\theta}_D/\dot{\theta}_S$  for subject T.W. in Figure 18 were used. Example #1 is an airplane travelling at 140 mph, 2000 ft from a runway 100 ft wide. If the pilot (subject T.W.) looked at the runway for 1.0 sec,  $\dot{\theta}_D/\dot{\theta}_S$  would equal 0.16, so that allowing for geometric factors (Figure 19), changing-size would be 76 times more effective than changing-disparity as a stimulus for motion-in-depth.

Example #2 is a cricket ball 2.5" in diameter 50 ft from the head and approaching at 90 mph. If subject T.W. inspected this rapidly-moving object for 0.25 sec, then from Figure 18,  $\dot{\theta}_D/\dot{\theta}_S$  would equal 0.47. Allowing for geometric factors (Figure 19), changing-disparity would be 2.1 times more effective than changing-disparity as a stimulus for movement-in-depth. Example #3 is a fly 0.2 cm wide moving at  $5 \text{ cm sec}^{-1}$  directly towards the head and located 50 cm from the head. If subject T.W. inspected the fly for 1.0 sec, then from Figure 18,  $\dot{\theta}_D/\dot{\theta}_S$  would equal 0.44. Allowing for geometric factors (Figure 19) changing-disparity would be 72 times more effective as a stimulus for movement in depth.

### Method of calculation

#### Example #1 Airplane

At 2000 ft the angular width of the runway is  $2.72^\circ$ . After 1 sec approaching at 140 mph, the angular width increases to  $3.02^\circ$ . Hence the mean rate of change of angular width  $\dot{\theta}_S = 0.295^\circ/\text{sec} = 17.7 \text{ min arc/sec}$  (i.e.  $8.86 \text{ min arc/sec}$  for each edge).

For subject T.W. the rate of change of disparity ( $\dot{\theta}_D$ ) equivalent to  $\dot{\theta}_S = 17.7 \text{ min arc/sec}$ , for an inspection time of 1.0 sec is  $\dot{\theta}_D = 1.4 \text{ min arc/sec}$ . (From Fig. 18).

$$\text{Hence } \dot{\theta}_D/\dot{\theta}_S = 0.16.$$

From the geometrical considerations outlined in Figure 19 we would expect that  $\dot{\theta}_D/\dot{\theta}_S = I/S$ . In this case  $S = 100 \text{ ft}$  and  $I = 2.5 \text{ inches}$ , as the geometrically predicted ratio  $\dot{\theta}_D/\dot{\theta}_S$  is 0.0021.

Hence, allowing for geometric factors, changing-size would be 76 times more effective than changing-disparity as a stimulus for motion-in-depth, for subject T.W.

#### Example #2 Cricket Ball

At 50 ft the angular width of the cricket ball is  $10.8 \text{ min arc}$ . After 0.25 sec approaching at 90 mph, the angular width increases to  $21.2 \text{ min arc}$ . Hence the mean rate of change of angular width  $\dot{\theta}_S = 42.4 \text{ min arc/sec}$  (i.e.  $21.2 \text{ min arc/sec}$  for each edge).

For subject T.W. and for an inspection time of 0.25 sec the rate of change of disparity ( $\dot{\theta}_D$ ) equivalent to  $\dot{\theta}_S = 42.4 \text{ min arc/sec}$  is  $\dot{\theta}_D = 10 \text{ min arc/sec}$ . (From Figure 18.)

$$\text{Hence } \dot{\theta}_D/\dot{\theta}_S = 0.47.$$

From the geometrical considerations outlined in Figure 19 we would expect  $\dot{\theta}_D/\dot{\theta}_S = I/S$ . In this case  $S = 2.5 \text{ inches}$  and  $I = 2.5 \text{ inches}$ , so the geometrically expected ratio  $\dot{\theta}_D/\dot{\theta}_S$  is 1.0.

Hence, allowing for geometric factors, changing-disparity would be 2.1 times more effective than changing-size as a stimulus for motion-in-depth for subject T.W.

#### Example #3 Fly

At 50 cm the angular width of the fly is  $13.1 \text{ min arc}$ . After approaching at 5 cm/sec for 1.0 sec, the angular width increases to  $14.5 \text{ min arc}$ . Hence the mean rate of change of angular width  $\dot{\theta}_S = 1.37 \text{ min arc/sec}$  (i.e.  $0.68 \text{ min arc/sec}$  for each edge).

For subject T.W. and for an inspection time of 1.0 sec the rate of change of disparity ( $\dot{\theta}_D$ ) equivalent to  $\dot{\theta}_S$  is equal to  $1.37 \text{ min arc/sec}$  is  $\dot{\theta}_D = 0.3 \text{ min arc/sec}$ . (From Figure 18.)

$$\text{Hence } \dot{\theta}_D/\dot{\theta}_S = 0.44.$$

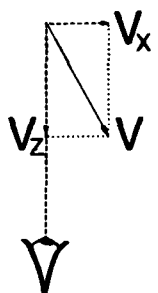
From the geometrical considerations outlined in Figure 19 we would expect  $\dot{\theta}_D/\dot{\theta}_S = I/S$ . In this case  $S = 0.2 \text{ cm}$  and  $I = 6.5 \text{ cms}$  as the geometrically expected ratio  $\dot{\theta}_D/\dot{\theta}_S$  is equal to 31.8.

Hence, allowing for geometric factors, changing-disparity would be 72 times more effective than changing-size as a stimulus for motion-in-depth for subject T.W.

The changing-size channel precisely computes the z-direction motion component independently of the x-direction motion component

Figure 20

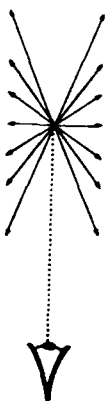
A



In the experiments described up to this point, we have shown that the human visual system contains a channel for pure antiphase oscillations (i.e. pure z-direction motion, see Fig. 20A). These experiments were restricted, however, since we used only pure antiphase and pure inphase stimuli (i.e. pure z-direction and pure x-direction motion). In the real world, of course, motion can occur along trajectories other than those along the z- and x-directions. We therefore carried out experiments to find: (a) whether the visual pathway precisely computes the x-direction component of motion ( $V_x$ )

for any arbitrary trajectory; (b) whether the visual pathway precisely computes the z-direction component of motion ( $V_z$ ) for any arbitrary trajectory.

B



The rationale of Experiment #1 is set out in Figure 20B where 7 different oscillation trajectories are shown. Each of these trajectories had the same x-axis component  $V_x$ . On separate days subjects adapted to each of these trajectories and we measured threshold elevations for pure x-direction and for pure z-direction test stimuli. If the visual pathway contained a channel for  $V_x$  that was independent of the value of  $V_z$ , then all 7 trajectories should give the same threshold elevation for the pure x-direction (inphase) test stimulus.

We found that this was not true. Inphase threshold elevations collapsed when even a small amount of z-axis motion was present (Fig. 21).

Figure 2

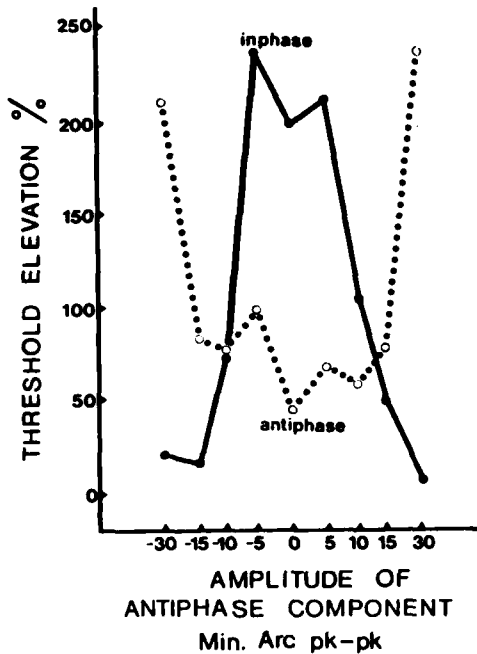
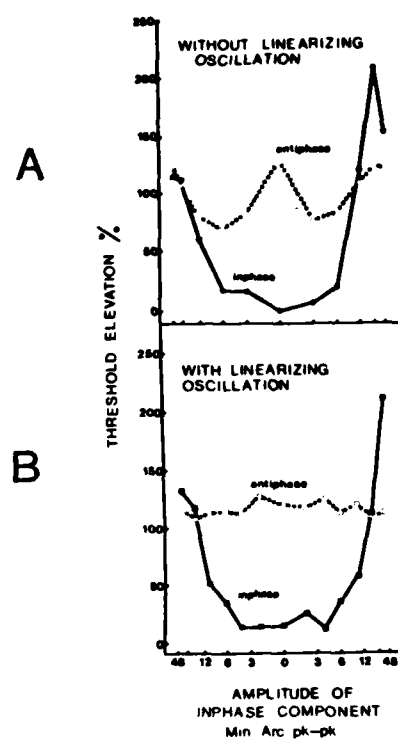


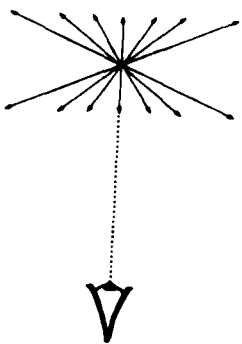
Figure 22



The rationale of Experiment #2 is set out in Figure 20C where 7 different trajectories are shown. Each of these trajectories had the same z-axis component

Figure 20

C



of motion ( $V_z$ ). On separate days subjects adapted to these trajectories, and we measured threshold elevations for z-direction (pure antiphase) and for x-direction (pure inphase) motion. If the changing-size channel does indeed compute z-direction motion ( $V_z$ ) accurately for any trajectory, then all the different trajectories should give the same threshold elevations for the antiphase test oscillation. Figure 22A shows that was approximately the case. Threshold elevations for the z-direction test stimulus were constant to within 30% even when x-direction oscillation of up to 8 times the amplitude of the z-direction motion was added to the adapting stimulus.

We conclude that the changing-size channel is independent of trajectory and acts as though it computes the algebraic difference between the velocities of an



object's opposite edges (i.e. when the edges move in opposite directions it adds the speeds, and when the edges move in the same direction it subtracts the speeds).

We noted that departure from constance was greatest for trajectories where two of the stimulus rectangle's sides were stationary. This suggested that the changing-size channel's 30% departure from accuracy might be a form of "crossover distortion". In which case, just as a high-frequency oscillation linearizes the crossover distortion in a magnetic tape recorder, an auxiliary linearizing oscillation might linearize the performance of the human visual system. We therefore repeated Experiment #2, but this time with a high-frequency (8 Hz) triangular wave linearizing oscillation added to the 2-Hz adapting oscillation as illustrated in Figure 23. Figure 22B shows that indeed the effect of the added 8-Hz oscillation was to abolish the 30% inaccuracy of the changing-size channel. In Figure 22B the changing-size channel computes the  $V_z$  component of motion to a remarkable accuracy of 5% for all trajectories tested. We note that the presence of linearizing oscillation can be regarded as typical of real-world viewing conditions (i.e. added "jitter" or vibration). The data of Figure 22A are replotted in polar coordinates in Figure 24 and the data of Figure 22B are replotted in Figure 25.

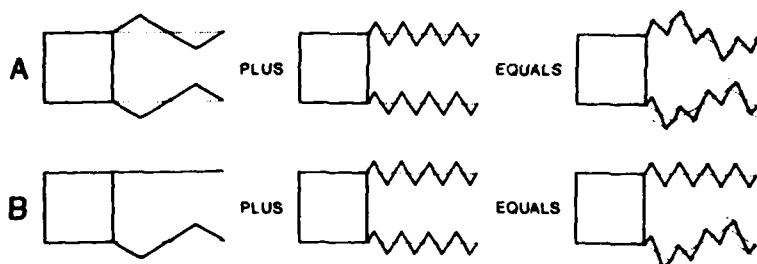


Figure 23

Oscillations of the edges of the stimulus for two trajectories "A" and "B". The trajectory "A" is directed along a line straight at the eye. For trajectory "B" one edge only just hits the eye. The rightmost squares show the 2-Hz oscillation with added 8-Hz linearizing oscillation.

Our finding implies that a small degree of "jitter oscillation" due, for example, to vibrations of the head or body considerably improves the performance of the human changing-size channel, and thus presumably improves the accuracy of motion-in-depth judgements.

#### WITHOUT LINEARIZING OSCILLATION

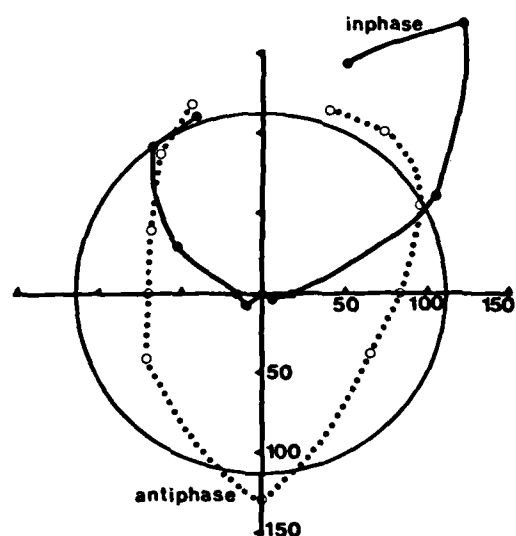


Figure 24

Dotted line shows sensitivity of z-direction motion channel for different trajectories. Without linearization.

#### WITH LINEARIZING OSCILLATION

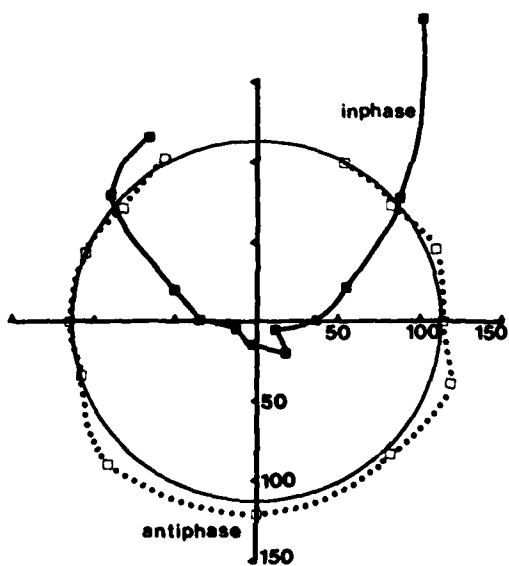


Figure 25

Dotted line shows sensitivity of z-direction motion channel for different trajectories. (With linearizing vibration or "jitter".)

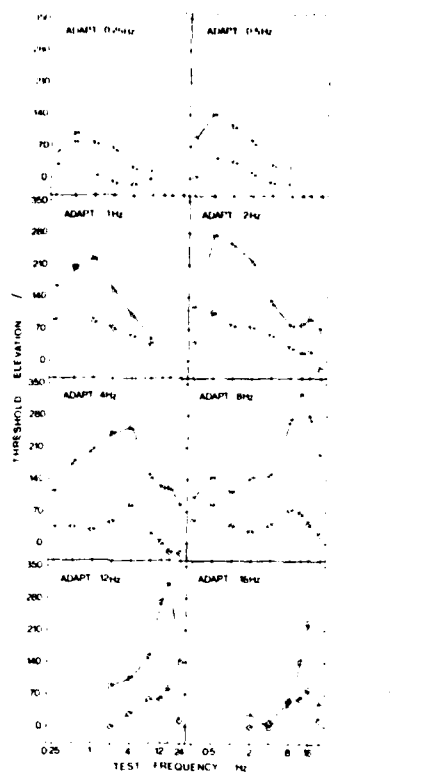


Figure 26

Temporal tuning of the changing-size channel.



### Dynamics of the changing-size channel

In order to understand how eye-limb coordination is limited in its dynamic performance it is necessary to measure the dynamic properties of each of the several visual channels involved in eye-limb coordination. Therefore we have investigated the temporal frequency response of the changing-size channel. In these experiments subjects adapted to a changing-size square of side length 0.5° whose size oscillated at F Hz, each size moving through 6 min arc pk-pk. Threshold for inphase and antiphase oscillations were measured before and adaptation for test frequencies of 0.25, 0.5, 1.0, 2.0, 4.0, 8.0, 12.0, 16.0 and 24 Hz. This experiment was repeated for adapting frequencies of 0.25, 0.5, 1.0, 2.0, 4.0, 8.0, 12.0 and 16.0 Hz. A total of 13 subjects were tested who worked 92 hours in total.

Figure 26 collapses data across all subjects. Percentage threshold elevation versus stimulus test frequency is plotted for each adapting frequency. We tentatively split the data into two frequency regions, namely 0.5-8.0 Hz and 8.0-16 Hz. Threshold elevations show clear temporal tuning in both frequency ranges. Clearly there is a plurality of frequency-selective subsystems: it is not the case that all changing-size channels have the same frequency selectivity. Between 0.5 and 8.0 Hz there are at least three and possibly a continuum of different frequency selectivities. Above 8.0 Hz there seems to be one sharply-tuned subsystem, peaking at 16 Hz.

Progress October 1, 1981 - September 30, 1982

Aims 1, 2, 3: Can subjects use flow pattern information to guide self-motion in the presence of retinal image translation caused by eye rotation and vehicular motion?

Gibson suggested that subjects can use the expanding visual flow pattern to guide self-motion. Figure 27 illustrates the point that translational motion of the retinal image can distort the flow pattern to the extent of shifting or even abolishing the focus.<sup>32-34</sup> Although Gibson discussed flow patterns, not on the retinal image, but in a theoretical construct (the "optic array") the central practical question remains: can subjects in practice use the flow pattern to guide self-motion in the presence of translational motion of the retinal image? Such translational motion would occur whenever the subject fixates a point in the external world other than the (presumably unknown)

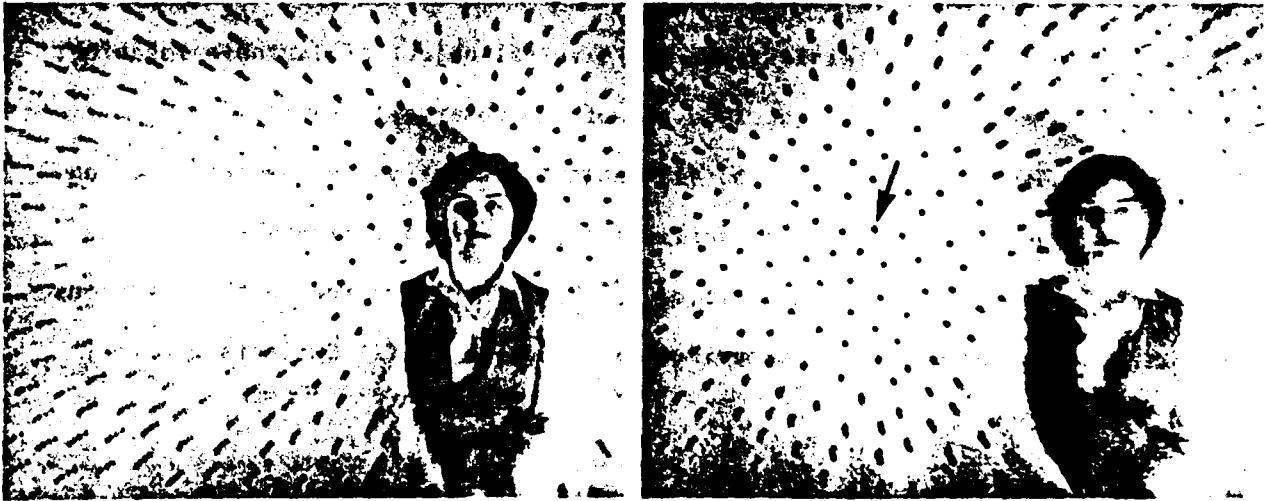


Fig.27 Expanding flow patterns similar to those in the retinal image for an observer moving through the outside world. Multiple exposure (left) was taken with a camera moving toward the girl's head while pointing directly at the head. Multiple exposure (right) was taken with a camera moving toward the head while pointing to one side (arrow). The center of the expanding flow pattern did not coincide with the direction of motion, but with the direction of the camera's "gaze."



destination and also when the vehicle (e.g. aircraft or helicopter) yaws, pitches or sideslips. Gibson also pointed out and discussed extensively that when an observer moves through the external world the image in the optic array is geometrically distorted, and suggested that this distortion is an aid to judging self-motion. It seems, however, that he did not explicitly distinguish between the effectiveness and reliability of expanding flow pattern and geometrical distortion as aids to judging self-motion. In particular, we note that translational motion has comparatively little effect on distortion in the retinal image. The equipment described below was designed to isolate and separately study the expanding flow pattern and geometrical distortion as aids to judging self-motion.

We developed a computer program to display on a CRT screen a dynamic image that mimicked the retinal image seen by an observer moving forwards towards a vertical plane.<sup>34</sup> In particular, the following parameters were included:

- (a) variable expanding flow pattern;
- (b) variable translational velocity;
- (c) variable geometrical distortion;
- (d) external object of variable location;
- (e) fixation mark to define the location of the observer's fovea.

Our findings were as follows: (1) Subjects cannot judge the centre of an expanding flow pattern in the presence of translational motion when there is no accompanying geometrical distortion.<sup>34</sup> This finding agrees with a previous report in a rather different experimental situation;<sup>33</sup> (2) Subjects are very

sensitive to geometrical distortion of the retinal image, and can accurately judge the location of the maximum rate of object magnification even in the presence of translational motion (Figs 28 & 29). The relevance of this finding to aviation is that in some\* (but not all) visual environments the maximum rate of change of magnification approximates the observer's destination. To give an impression of the dynamics, we can say that our experimental conditions approximated the view from an automobile travelling at 30 mph directly at a wall 80 yards away.

---

\* For example, an observer travelling at right angles to a flat plane as in a steep dive.

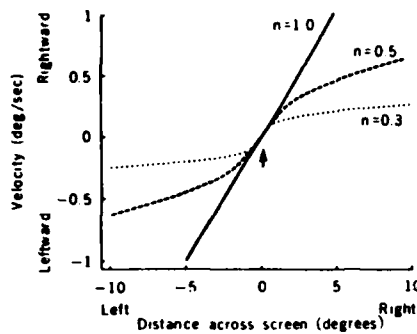
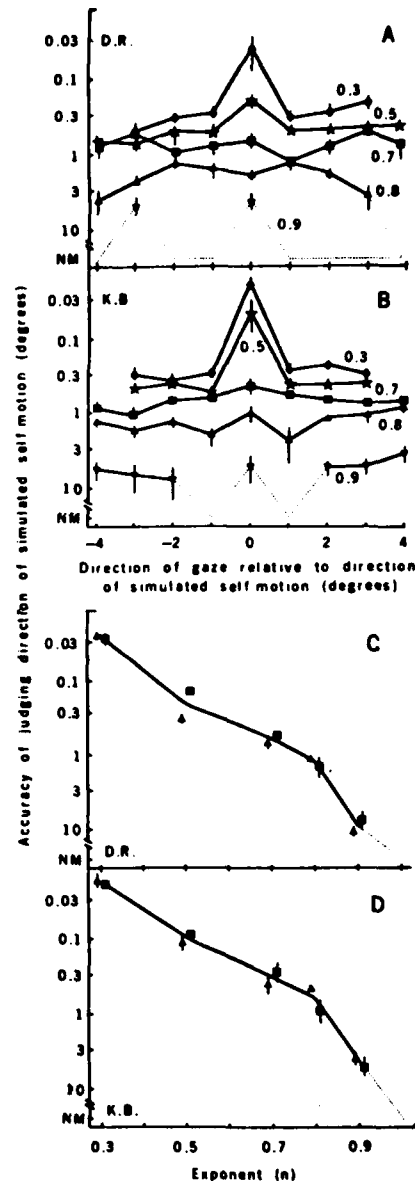


Fig. 28 (above). Three of the expanding flow patterns used in this study. The instantaneous velocity at any point in the pattern was first made a power function of distance across the pattern. Then a uniform translational speed was added to render stationary the pattern at the center of the screen (the point of gaze). Solid line, expansion pattern for which the rate of change of magnification was uniform across the pattern ( $n = 1.0$ ). Dashed line, rate of change of magnification was slightly greater at one point in the pattern (arrow) than elsewhere ( $n = 0.5$ ). Dotted line, rate of change of magnification was considerably greater at the arrow than elsewhere ( $n = 0.3$ ). In different stimulus presentations the point of maximum rate of magnification occurred at the center of the screen or at various distances to left and right of center, but the pattern at the center of the screen was always stationary.

Fig. 29 (right). (A and B) Subjects were not able to disentangle the direction of gaze from the direction of self motion when the rate of change of spatial frequency was uniform over the pattern ( $n = 1.0$ ) and could hardly perform the task for  $n = 0.9$ , but when the rate of change of magnification was appreciably greater along the direction of simulated self motion, subjects were able to judge the direction of simulated self motion almost independently of the direction of gaze ( $n = 0.8, n = 0.7$ ). For  $n = 0.5$  and  $n = 0.3$ , subjects were somewhat more accurate when looking approximately along the direction of simulated self motion. The rate of expansion in all cases was equivalent to impact with the target 5 seconds after onset of stimulation. Initial spatial frequency, 5 cycle/deg. Field size, 16° vertical by 20° horizontal; mean luminance, 30 cd/m<sup>2</sup>; and viewing was monocular. (C and D) Accuracy measured with subjects looking approximately along the direction of motion.



Figures 28 and 29

Aims 1, 2: Texture changes versus size changes as stimuli for motion in depth

Many real-world objects that have a definite boundary also have a visible surface texture. The retinal image of such an object continuously undergoes two types of change as it approaches; the image size grows larger and the surface texture grows coarser. We compared these two visual changes in terms of their effectiveness as stimuli for the sensation of motion in depth. We attempted to dissociate their contributions to the sensation of motion in depth by pitting one against the other.<sup>35</sup> For this purpose we developed special-purpose electronics controlled by computer that can display the textured patterns on a CRT. Figure 30 illustrates several combinations of texture change and size change.

We used the strength of the motion in depth aftereffect as an index of the effectiveness of any stimulus. The motion in depth aftereffect was measured in exactly the same way for all the different stimuli, namely by cancelling the aftereffect using a blank square as test stimulus.

We found that changing the size of an untextured object is an effective stimulus for motion in depth, as indicated by the stars at zero on the abscissae in Figure 31. This effectiveness was strikingly reduced by the presence of static texture. Figure 32 shows how progressively raising the contrast of static texture from zero progressively reduced the strength of the motion in depth aftereffect almost to zero.

Changing texture alone with constant square size was a fairly effective stimulus for motion in depth as indicated by the dashed lines in Figure 31, whereas changing stimulus object size with static texture is comparatively ineffective (intersection of the continuous line plots with the ordinates).

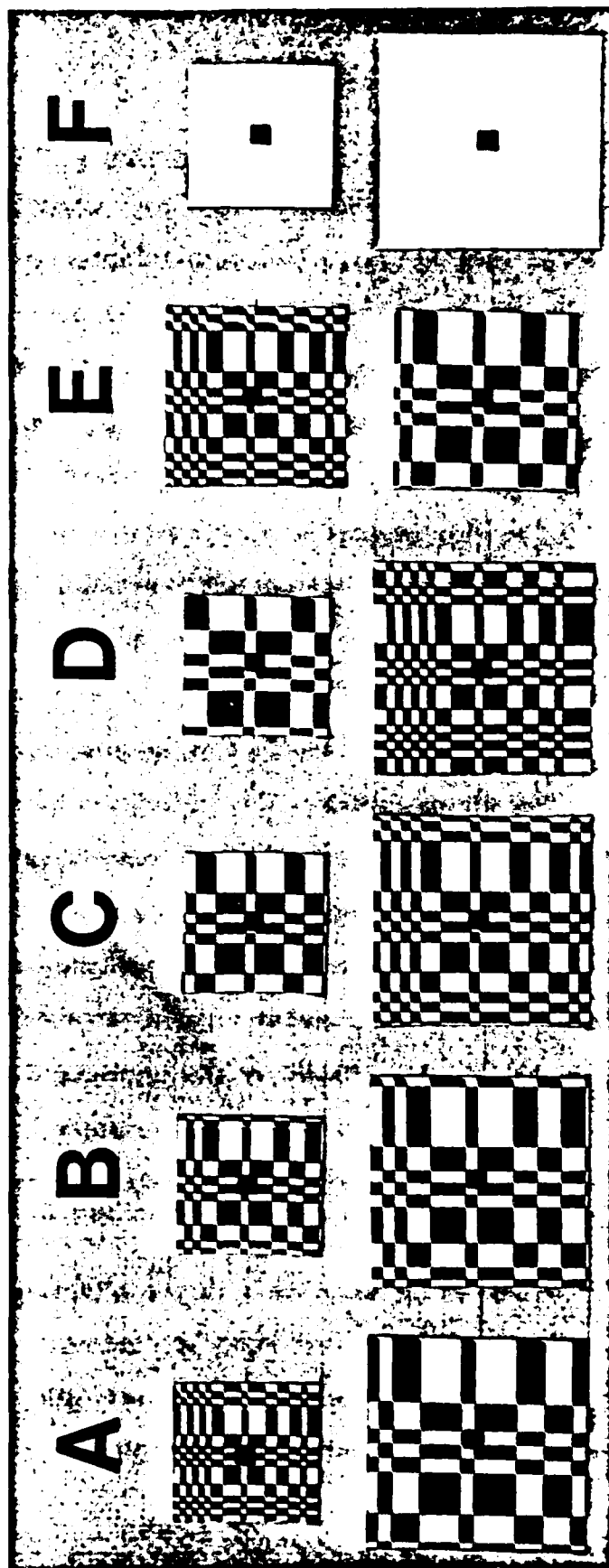


Figure 30. Examples of adapting and test stimuli at the start and end of the presentation ramp. A through F show different adapting stimuli. The test stimulus was always as shown in F. In A, square size contracted at a rate of 17.4 min arc sec<sup>-1</sup> while texture size contracted at a rate of 34.8 min arc sec<sup>-1</sup>. In B, square size and texture size both contracted at a rate of 17.4 min arc sec<sup>-1</sup>. This stimulus corresponded to a real-world target whose magnification was changing. In C, square size contracted at a rate of 17.4 min arc sec<sup>-1</sup> while texture size was constant. In D, square size contracted at a rate of 17.4 min arc sec<sup>-1</sup> while texture size expanded at a rate of 17.4 min arc sec<sup>-1</sup>. In E, square size was constant while texture size contracted at a rate of 17.4 min arc sec<sup>-1</sup>. The min arc sec<sup>-1</sup> values are for a presentation duration of 1.7 sec and mean square side length of 1.2°. These illustrations are photographs of the CRT display used in this study.

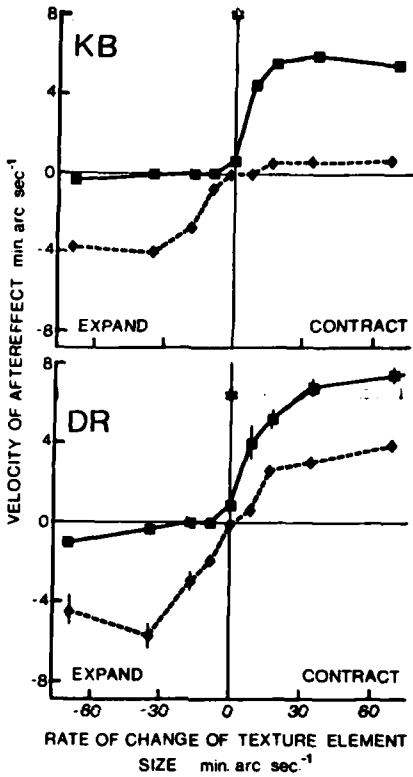
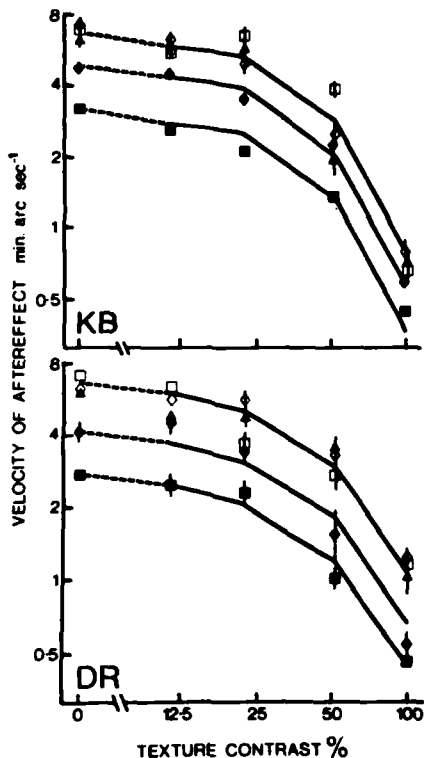


Figure 31. Motion-in-depth produced by texture alone, by size, and by texture plus size. A motion-in-depth aftereffect was produced by inspecting a textured square of  $1.2^\circ$  mean side length that contracted with a ramping waveform. The adapting square's texture contracted at different rates (illustrated in Figure 30A, B and plotted as positive abscissae) or expanded at different rates (illustrated in Figure 30D and plotted as negative abscissae). Ordinates plot the rate of change of the test square's side length required to just cancel the motion-in-depth aftereffect (continuous lines). The test square was always untextured. Filled diamonds (dashed lines) plot the strengths of aftereffects produced by inspecting a textured square whose side length was a constant  $1.2^\circ$ , but whose texture element size expanded or contracted at different rates (e.g. Figure 30E). Dashed lines plot the strength of this aftereffect. The stars at zero on the abscissa show the strength of the motion-in-depth aftereffect produced by inspecting the untextured adapting square shown in Figure 30F. The vertical extent of the horizontal shaded area indicates  $\pm 1$  SE. Vertical lines show  $\pm 1$  SE. Where absent they were smaller than the symbol. Each point is the mean of 10 settings.



**Figure 32.** Effect of texture contrast on the motion-in-depth aftereffect. The rate of change of the test square's side length required to just cancel the motion-in-depth aftereffect (ordinates) was measured as a function of the "texture contrast" of the adapting square (abscissa). The test square was always untextured. The curve was measured for a mean square contrast of 200% (open squares) and for 100% (open diamonds), 50% (open triangles), 25% (filled diamonds), and 12.5% (filled squares). All the data points were taken into account in deriving a single curve. This single curve was bodily shifted along the logarithmic ordinate to give the best (least square) fits shown. Vertical lines show  $\pm 1$  SE. Where absent they were smaller than the symbol. Each point is the mean of 10 settings. "Texture contrast" was defined equal to  $100(c/a)\%$ . "Square contrast" was defined equal to  $100(a/b)\%$ . A and B show data for subjects KB and DR respectively.

What is the relative effectiveness of these two stimuli for motion in depth when both are present simultaneously? The continuous line in Figure 31 plots the strength of the motion-in-depth aftereffect when both stimuli were present, sometimes acting in conjunction (positive abscissae), and at other times being pitted against one another (negative abscissae).

With the aim of dissociating the parts played by texture changes and by expansion of object size as stimuli for motion in depth we write

$$d = \frac{(\text{magnitude of measured aftereffect}) - (\text{magnitude of predicted aftereffect})}{(\text{magnitude of measured aftereffect}) + (\text{magnitude of predicted aftereffect})}$$

$$= \frac{|A_{S+T}| - |A_S + A_T|}{|A_{S+T}| + |A_S + A_T|}$$

where  $d$  is the summation ratio,  $A_{S+T}$  is the strength of the aftereffect when both square size and texture element size change,  $A_S$  is the strength of the aftereffect when only square size changes, texture element size being constant, and  $A_T$  is the strength of the aftereffect when only texture element size changes, square size being constant. Values of  $d$  calculated from the Figure 31 data plotted in Figure 33 shows that, in almost all cases, the aftereffect produced by simultaneous changes of size and texture was not simply the sum of the separate aftereffects produced by size change alone and by texture change alone. In other words  $d$  was not equal to zero in most stimulus conditions. Figure 33 shows that when square size and texture element size both contracted, the departure from linear summation was in the direction of enhanced motion-in-depth aftereffect ( $d > 0$ ). This enhancement could be so large that the recorded aftereffect ( $A_{S+T}$ ) was 6.6 times greater than ( $A_S + A_T$ ), the sum of the two separate contributions (subject KB at +1 on the abscissa). However, when square

size contracted while texture element size expanded, the departure from linear summation was in the direction of reduced aftereffect ( $d < 0$ ). This mutual inhibition could be so great that no aftereffect ( $A_{S+T}$ ) at all could be recorded (-1 and -2 on abscissa for both subjects), even though the linearly-predicted aftereffect ( $A_S + A_T$ ) was large. The striking influence of this interaction between texture and size contributions is illustrated by noting that, for subject KB, the sum of the two contributions ( $A_S + A_T$ ) was rather larger at -2 on the abscissa ( $A_S + A_T = 11.5$ ) than at +4 on the abscissa ( $A_S + A_T = 7.3$ ), yet no aftereffect at all was recorded in the first case ( $A_{S+T} = 0$ ) while the second condition produced the strongest recorded aftereffect.

Due to current limitations in computer-generated imagery (CGI) techniques, almost all commercially available flight simulators represent the visual world in a cartoon-like fashion so that an object's limiting boundary is shown, but surface texture is almost or completely absent. However, there are CGI simulator displays under development that include some texture and shading. Our emphasis here on dynamic features of vision departs somewhat from the emphasis on static picture quality (e.g. as would be seen in a still photograph of one TV frame) that has traditionally been the chief criterion of quality in simulator displays. Here we report evidence that texture dynamics are important in motion-in-depth perception, since strong interactions can occur between visual responses to changing texture and to changing size. In terms of the monocular, two-dimensional simulation of motion in depth, our findings suggest that in most conditions the presence of texture reduces stimulus effectiveness, and at best the presence of texture adds little to the effectiveness of an untextured stimulus (Figure 32).

more than sum

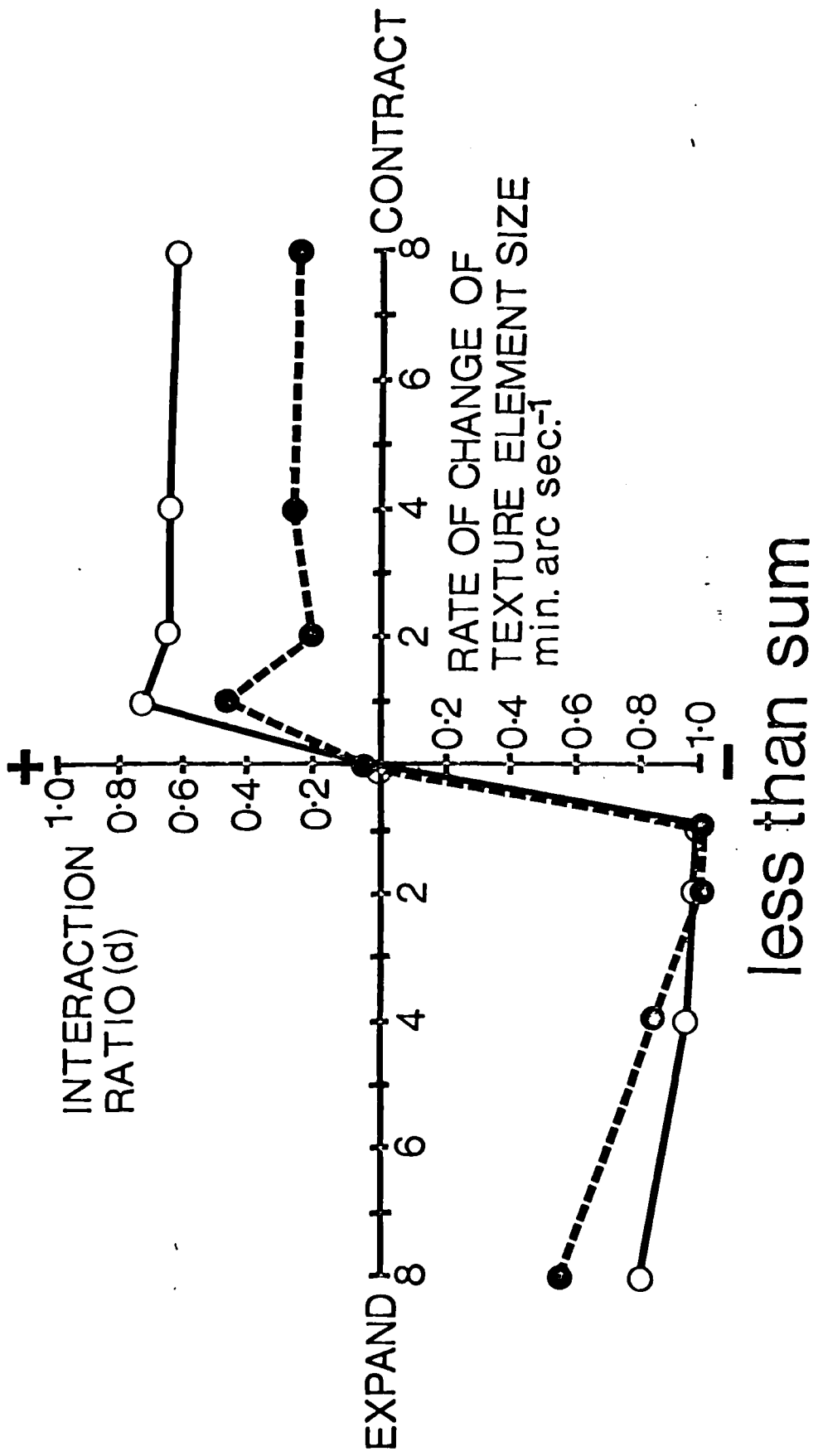


Figure 33. Interaction between responses to texture and to size. The strength of the interaction ( $d$ ) between size and texture in the Figure 31 data (ordinates) was plotted versus the rate of change of texture element size (abscissa). Since adapting square size contracted, texture element size changes in the same direction for positive abscissae, but changed antagonistically for negative abscissae. " $d$ " was defined by the equation  $d = \frac{|A_{S+T}| - |A_S + A_T|}{|A_{S+T}| + |A_S + A_T|}$ , where  $A_{S+T}$  was the aftereffect strength produced by a combination of size change and texture change,  $A_S$  was the aftereffect strength produced by size change alone, the adapting stimulus being textureless, and  $A_T$  was the aftereffect strength produced by texture change alone, the adapting square being of unvarying size. Positive and negative values of  $d$  mean that the magnitude of the measured aftereffect  $A_{S+T}$  was respectively larger and smaller than the sum of the separate texture and size contributions. Open circles (continuous line) and closed circles (dashed line) plot data for subjects KB and DR.

Aims 1, 2: Brain neurons that may underlie the motion-in-depth channels in man

We have found single-neuron evidence to support our proposal that the visual pathway has separate stereoscopic subsystems tuned to relative position in depth and to the direction of motion in depth. We used extracellular micro-electrodes to record from single neurons in the visual cortex of anaesthetized cat.<sup>36,37</sup> Figure 34A shows a class of binocular neuron that is so sharply tuned to the direction of motion in depth that it responds to a range of directions in depth spanning only 1° to 2°. The neuron of Figure 34A accurately maintained its tuning over a fourfold range of speeds.<sup>36</sup> Some of these neurons are comparatively unaffected by disparity over a disparity range of several degrees.<sup>37</sup> These neurons are very sensitive to motion in depth while being little affected by position in depth. Figure 34B shows a different type of neuron that responds only over a narrow range of disparities. This type of "binocular depth" neuron was well known previously. Figure 34B, however, adds the finding that this depth neuron is also tuned to the direction of motion in depth, since it fires strongly only for motion in the frontal plane.

Aims 1-3: Theoretical and practical development of the channel theory and its relevance to aviation

The channel hypothesis reviewed in "Background" above has been developed more extensively in an article for Psychological Review,<sup>38</sup> and the implications for skilled eye-limb coordination are surveyed in an invited Festschrift for Professor I. Köhler.<sup>39</sup>

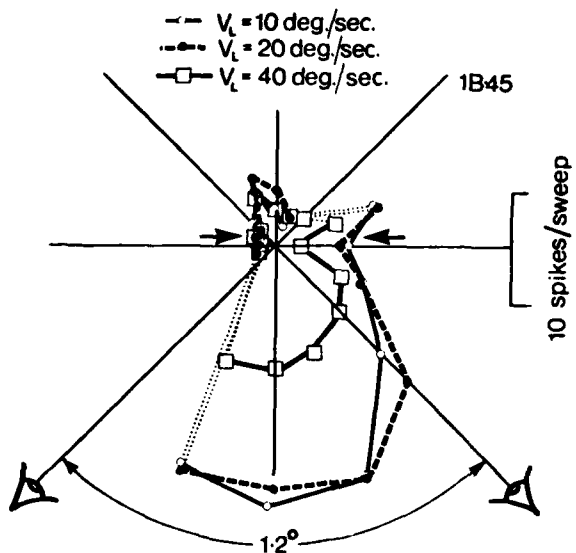


Figure 34A

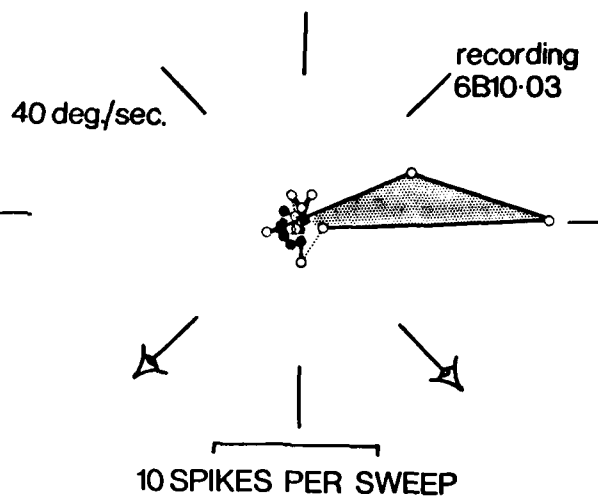


Figure 34B

Spikes recorded from single neurons in cat visual cortex (plotted radially) as a function of the direction of motion in depth (plotted as azimuthal angle).

A - This unit maintains its very selective tuning to the direction of motion in depth over a 4:1 speed range. Note that firing is almost restricted to a range of directions little wider than  $1^\circ$ . This directional tuning is achieved by interocular inhibition as shown by the arrows.

B - This unit fired appreciably only when the target moved closely parallel to the frontoparallel plane in a left-right direction and when vision was binocular. Closed circles show firing when the two eyes were stimulated separately and open circles show firing when binocular vision was used. The dotted area indicates the very strong interocular facilitation observed for binocular vision.

Aims 4, 6, 7: Correlations between visual test results and flying performance on the Advanced Simulator for Pilot Training (ASPT)

This work was carried out at Williams AFB in two visits. It was a joint effort by Mr. R. Kruk (who conducted the measurements at Williams AFB), Dr. T. Longridge of Williams AFB/HRL, Dr. K. I. Beverley (Dalhousie) and Dr. D. Regan (P.I.). This work could not have been carried out without the expert aid and advice of the staff of HRL, Williams AFB and the expert aid and cooperation of student pilots and pilot instructors (82nd, 96th and 97th FTS, Williams AFB), fighter pilots (429 TFS and 474 TFW, Nellis AFB, 62 TFTS and 56 TTS, MacDill AFB and weapons systems officers (58 TTS, Luke AFB).

First visit to Williams AFB

The aim of this visit was to correlate visual psychophysical and visual tracking test results both with simulator flying performance and with flying grades in aircraft. A battery of 13 test results was successfully obtained from each subject tested. The simulator tests chosen were low-visibility landing (ASPT simulator) and formation flying (formation simulator). Unfortunately, the formation simulator broke down, so we were restricted to landing data.

A multiple-staircase tracking method was used to obtain psychophysical data. Although this does not separate criterion from sensitivity as well as ROC methods, it is more satisfactory than the method of adjustment, and much faster than ROC methods. Tracking data for changing-size (motion in depth) perturbed changing-size (to reveal "crosstalk" between channels) and sideways motion were obtained using our device described elsewhere (Ref. 40 and the previous AFOSR report. This device has been patented by the Air Force.) The psychophysical tests are listed in Table 1. Each of the five groups tested comprised 12 members as follows:



Group 1 - Air Force primary student jet pilots training on the T37 aircraft;  
Group 2 - Air Force graduating student pilots training on the T38 aircraft;  
Group 3 - experienced pilot instructors;  
Group 4 - experienced weapons officers. This control group had a large number of flying hours comparable to the instructors, but differed in that they were not pilots;  
Group 5 - civilian, nonflying control subjects.

Visual test results are listed in Table 1.

Our main conclusions are as follows. For advanced student pilots (Group 2) good predictions of low-visibility landing performance, as assessed by the number of crashes, could be made on the basis of the antiphase tracking test.

Figure 35 illustrates this finding.

The distance from the runway threshold at which the pilot made his first flight correction correlated most strongly with the results of the inphase tracking test. In particular, the better the pilot performed on this test, the further he was from the runway when he made his first flight correction. This finding is illustrated in Figure 36.

At first sight it might seem surprising that we did not find strong correlations between any of our various contrast threshold tests and restricted-visibility landing performance. In extreme cases, very low contrast sensitivity must obviously produce poor landing performance since the pilot cannot see the runway until it is too late. Our finding can be understood if, in the particular groups studied, intersubject differences in contrast sensitivity were sufficiently small that they were not a dominant factor in landing performance. Nevertheless, this would not necessarily indicate that existing visual tests were always successful in detecting applicants with unduly low contrast sensitivities,

| TEST   | THRESHOLDS AND STANDARD DEVIATIONS |             |             |             |             | GROUP 5 |
|--|------------------------------------|-------------|-------------|-------------|-------------|---------|
|  | GROUP 1                            | GROUP 2     | GROUP 3     | GROUP 4     |             |         |
| Inphase oscillation threshold                                | SI<br>1.28 (0.18)                  | 1.12 (0.16) | 1.16 (0.23) | 1.14 (0.20) | 1.4 (0.26)  |         |
| Antiphase oscillation threshold                              | SA<br>0.96 (0.20)                  | 0.78 (0.12) | 0.90 (0.19) | 0.80 (0.14) | 1.12 (0.18) |         |
| Inphase osc. contrast threshold peripherally viewed square   | CPI<br>6.5 (0.76)                  | 6.5 (0.31)  | 6.7 (0.45)  | 6.4 (0.31)  | 6.5 (0.24)  |         |
| Antiphase osc. contrast threshold peripherally viewed square | CPA<br>6.6 (0.60)                  | 6.6 (0.36)  | 6.9 (0.61)  | 6.5 (0.35)  | 6.6 (0.31)  |         |
| Inphase osc. contrast threshold centrally viewed square      | CDI<br>6.2 (0.42)                  | 6.1 (0.18)  | 6.2 (0.28)  | 6.2 (0.37)  | 6.2 (0.30)  |         |
| Antiphase osc. contrast threshold centrally viewed square    | CDA<br>6.3 (0.52)                  | 6.2 (0.25)  | 6.4 (0.37)  | 6.4 (0.49)  | 6.5 (0.71)  |         |
| Grating contrast threshold                                   | G<br>27 (2.6)                      | 26 (3.2)    | 24 (2.4)    | 27 (4.7)    | 29 (2.6)    |         |
| TRACKING ERRORS  |                                    |             |             |             |             |         |
| Inphase tracking errors 0-0.25 Hz                            | TII<br>700 (220)                   | 1050 (450)  | 573 (150)   | 662 (300)   | 844 (300)   |         |
| Inphase tracking errors above 0.25 Hz                        | TI2<br>147 (16)                    | 147 (18)    | 145 (17)    | 145 (17)    | 166 (36)    |         |
| Antiphase tracking errors 0-0.25 Hz                          | TA1<br>263 (190)                   | 218 (110)   | 309 (270)   | 385 (420)   | 462 (280)   |         |
| Antiphase tracking errors above 0.25 Hz                      | TA2<br>141 (30)                    | 128 (18)    | 137 (20)    | 143 (16)    | 182 (24)    |         |
| Perturbed antiphase tracking errors 0-0.25 Hz                | TP1<br>283 (160)                   | 201 (82)    | 244 (91)    | 286 (240)   | 424 (270)   |         |
| Perturbed antiphase tracking errors above 0.25 Hz            | TP2<br>146 (28)                    | 138 (20)    | 150 (14)    | 134 (22)    | 178 (22)    |         |

Table 1

Group means and standard deviations for all psychophysical and tracking tests. SDs are bracketed. Tracking errors expressed as RMS values in arbitrary units. SI and SA in min arc peak-to-peak per edge. CEP, CPA, CDI, and CDA are in percent contrast. G is in dB attenuation where 0 dB is 25% contrast. (Note that 6 dB is a factor of two and 20 dB is a factor of 10, thus 20 dB here means 2.5% contrast.)

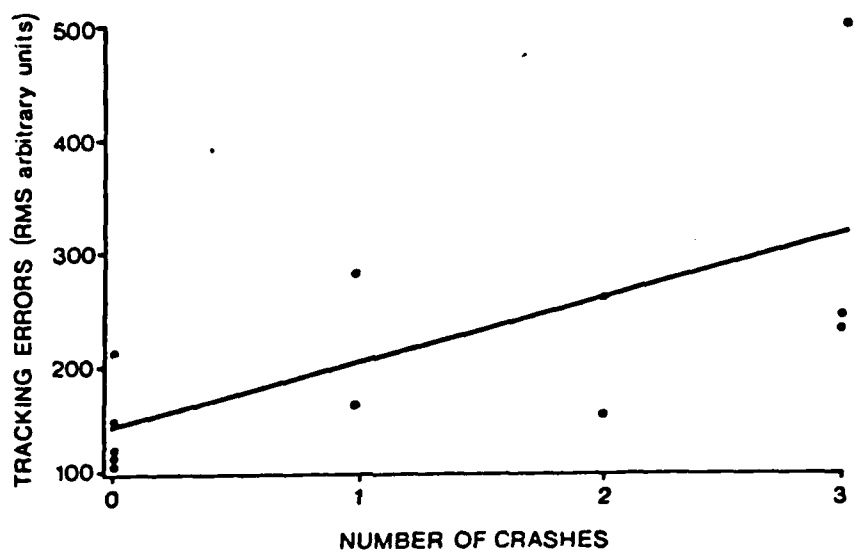
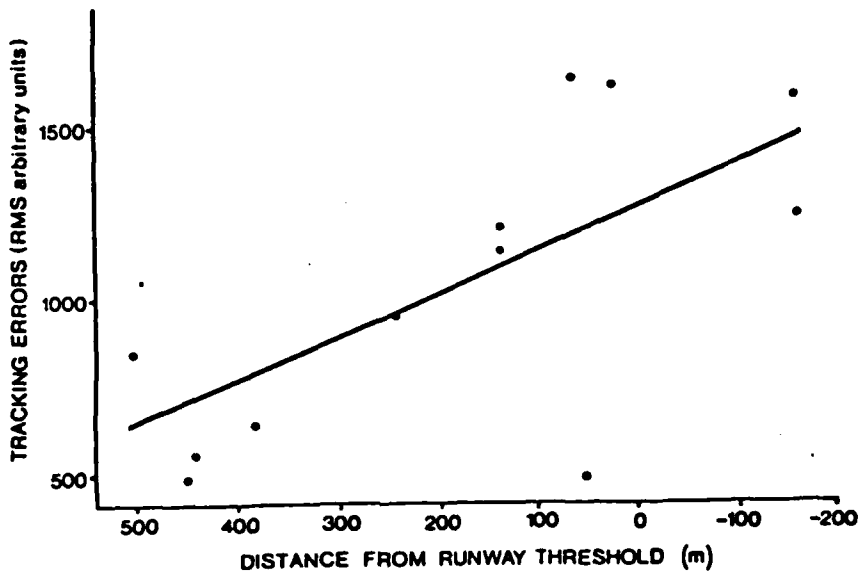


Figure 35

Relation between tracking performance and the number of crashes. Ordinates plot error in tracking a test square whose size continuously and unpredictably changed as though moving in depth. Errors in the frequency range below 0.25 Hz only are shown. Abscissae plot the number of crashes made in four low-visibility landings on the ASPT simulator (A-10 cockpit). Data for 12 graduating student pilots are shown (linear regression).

Figure 36

Relation between tracking performance and the distance from the runway threshold at which pilots made the first flight correction. Ordinates plot errors in tracking a test square that moved unpredictably in the frontoparallel plane. Errors in the frequency range below 0.25 Hz only are shown. Abscissae plot the distance from runway threshold at which the first flight correction was made. Negative distances mean that the pilot has passed over the threshold before his first correction. Results are the mean for four low-visibility landings on the ASPT simulator (A-10 cockpit). Data for 12 graduating student pilots are shown (linear regression).

but merely that our groups did not contain any individuals with 20/20 vision or better accompanied by very low contrast sensitivity. (As suggested by Dr. Ginsburg elsewhere, individuals with low contrast sensitivity could readily be detected by adding a contrast sensitivity test to the Snellen acuity test.)

On the other hand, it seems that motion-in-depth tracking and sideways motion tracking did measure some factor that is of dominant importance in restricted-visibility landings, and also shows considerable intersubject variability.

This research is described in Ref. 41 enclosed.

Second visit to Williams AFB

Although the conclusions drawn from the first visit were based on correlations that were statistically very significant we felt that re-running the study on a different occasion with different groups of pilots would be a useful check. Our main aim in this second study was to confirm or deny the conclusions of the first study.

However, we also took the opportunity to extend the scope of the study. We added an additional psychophysical test, namely visual sensitivity to an expanding visual flow pattern. This test measured ability to discriminate between slightly different rates of expansion. We tested a slow rate of expansion and a fast rate. We envisaged that high discrimination on this test might correlate with good simulator performance on, e.g., the diving/bombing task and on the formation flight task. For this test we used a portable version of a flow pattern stimulator described previously,<sup>28</sup> modified to be controlled by PET microcomputer using the psychophysical method of constant stimuli.

The simulator test was expanded to constitute a "mission" that included the following tasks: (1) formation flight with a second aircraft (six attempts);

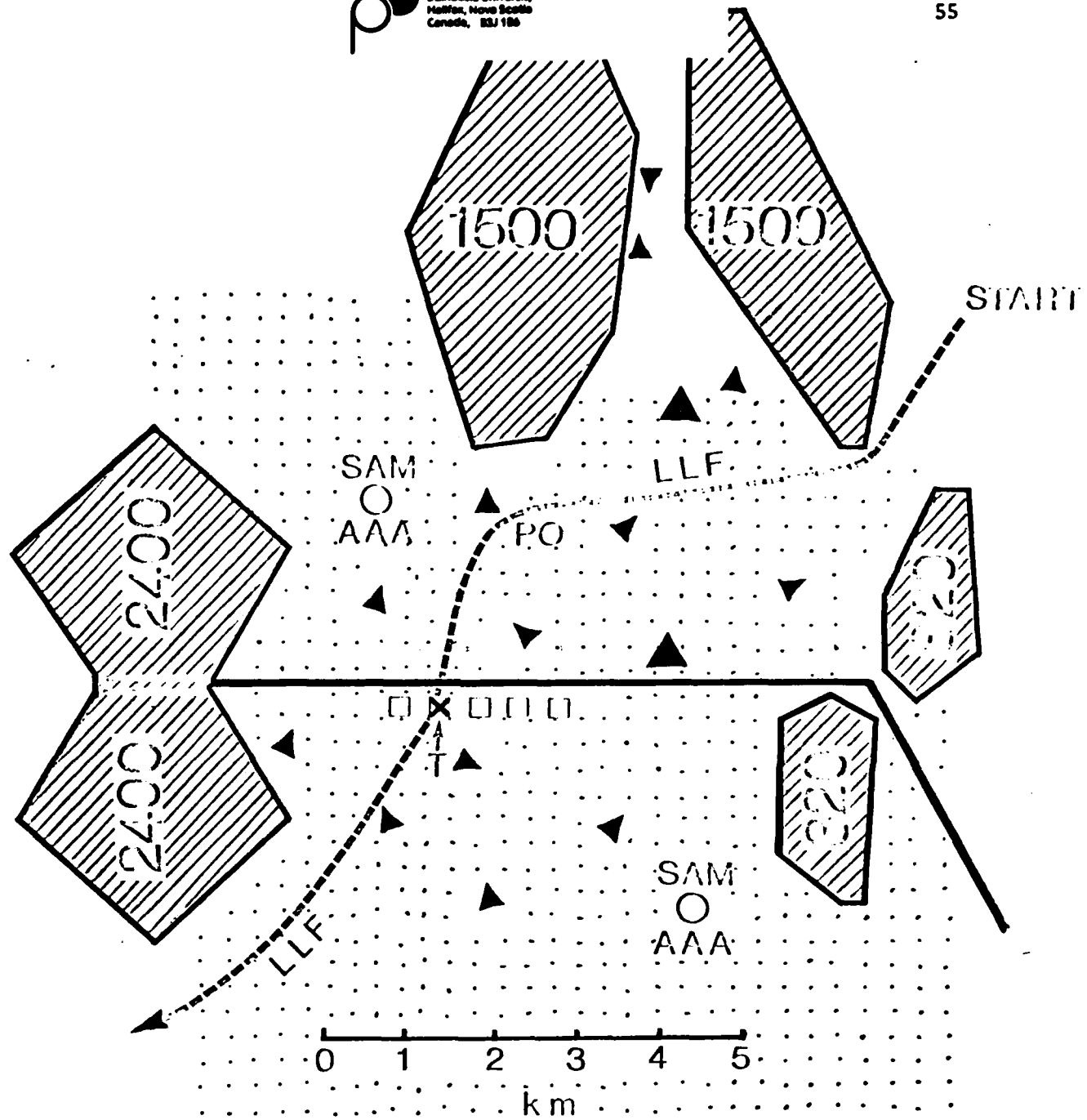


Figure 37. Environment in low-level flight task. Small dots indicate cones 13 m high and small triangles indicate 30 m pinnacles. Large triangles indicate 180 m hills. Mountains are shaded, heights given in meters. T marks target. SAM and antiaircraft artillery (AAA) marked. Dashed line shows approximate flight path. LLF - low-level flight. Approximate pop up point parked PO. Scale shows distance in kilometers.

(2) low altitude approach past AA guns and SAMs, pop-up, bomb delivery and exit (Figure 37); (3) restricted-visibility landings. Performance was measured on each task, and performance measures were successfully obtained for every subject tested.. A new group carried out the simulator test in addition to advanced student pilots and pilot instructors. The new group comprised 12 F-16 operational pilots.

Our main findings were as follows: Simulator flying performance was compared with the results of sensory visual tests for 12 student pilots, 12 instructor pilots and 12 fighter pilots and aircraft flying grades were compared for student pilots. Simulator tasks comprised formation flight, low-level flight, bombing and restricted-visibility landing. Visual tests comprised super-threshold velocity discrimination of a radially-expanding flow pattern, manual tracking of both motion in depth and motion in the frontal plane, motion thresholds and contrast thresholds for a moving square and a static sinewave grating.

Landing and formation flight performance correlated with both manual tracking and expanding flow pattern test results. Pilots who were better able to discriminate different rates of expansion of the test flow pattern achieved a greater percentage of hits and near misses in the low-level flight and bombing task. Aircraft flying grades for student pilots correlated with expanding flow pattern test results and with manual tracking of motion in depth. These findings suggest that tests of visual sensitivity to superthreshold motion might usefully be added to current selection tests for flying personnel. These findings also emphasize the importance of accurate, artifact-free representation of motion in simulator visual displays. These findings are in process of publication.<sup>42</sup>

Extension of simulator studies to real aircraft

We have extended the simulator findings to real aircraft by comparing our laboratory test results with flying performance in telemetry-tracked high performance jet fighters at the Yuma TACTS facility. (This study was made possible only by excellent cooperation with U.S. Marines, U.S. Navy and TACTS staff.) Pilots carried out two flying tasks using A4 and F-14 aircraft. These tasks were air-to-air combat and a low-level task comprising approach, pop up, and bomb delivery. Bombing accuracy was assessed for both no-drop computer scoring and also using real bombs. Results on our motion in depth tracking test and on our expanding flow pattern velocity discrimination task correlated with bombing accuracy and with success in air-to-air combat. Pilots also carried out two airborne visual tests. These comprised: (a) visual acquisition range; (b) visual judgement of whether the adversary aircraft was turning left or turning right. These test results also correlated with bombing accuracy and success in air-to-air combat. These findings are currently in preparation.



#### REFERENCES

1. Ogle, K.N. (1964) RESEARCHES IN BINOCULAR VISION. New York, Hafner.
2. Richards, W. (1975) Visual space perception. In HANDBOOK OF PERCEPTION, Vol. V.
3. Julesz, B. (1971) FOUNDATIONS OF CYCLOPEAN PERCEPTION, Chicago, Univ. of Chicago Press.
4. Barlow, H., Blakemore, C.B. and Pettigrew, J.D. (1967) The neural mechanism of binocular depth discrimination. J. Physiol., Lond. 193, 327-342.
5. Nikara, T., Bishop, P.O. and Pettigrew, J.D. (1968) Analysis of retinal correspondence by studying receptive fields of binocular single units in cat striate cortex. Exp. Brain Res. 6, 353-372.
6. Bishop, P.O. (1973) Neurophysiology of binocular single vision and stereopsis. In HANDBOOK OF SENSORY PHYSIOLOGY, Vol. VII/3A, Berlin, Springer.
7. Richards, W. (1972) Response functions for sine- and square-wave modulations of disparity. J. opt. Soc. Amer. 62, 907-911.  
Richards, W. (1973) Factors affecting depth perception. Air Force Office of Scientific Research report, AFOSR-TR-73-0439.



8. Beverley, K.I. and Regan, D. (1973) Evidence for the existence of neural mechanisms selectively sensitive to the direction of movement in space. *J. Physiol., Lond.* 235, 17-29.
9. Richards, W. and Regan, D. (1973) A stereo field map with implications for disparity processing. *Invest. Ophthal.* 12, 904-090.
10. Cynader, M. and Regan, D. (1978) Neurons in cat parastriate cortex sensitive to the direction of motion in three-dimensional space. *J. Physiol., Lond.* 274, 549-69.
11. Beverley, K.I. and Regan, D. (1975) The relation between discrimination and sensitivity in the perception of motion in depth. *J. Physiol., Lond.* 249, 387-398.
12. Regan, D. and Beverley, K.I. (1978) Stereoscopic perception: different channels for motion and position. In FRONTIERS OF VISION RESEARCH (1977 Houston Symposium), Springer.
13. Regan, D., Beverley, K.I. and Cynader, M. (1979) Stereoscopic subsystems for position and for motion in depth. *Proc. Royal Soc.* 204, 485-501.
14. Regan, D. and Beverley, K.I. (1978) Looming detectors in the human visual pathway. *Vision Res.* 18, 415-421.
15. Regan, D. and Beverley, K.I. (1978) Illusory motion in depth: aftereffect of adaptation to changing size. *Vision Res.* 18, 209-212.
16. Beverley, K.I. and Regan, D. (1979) Visual perception of changing size: the effect of object size. *Vision Res.* 19, 1093-1104.
17. Beverley, K.I. and Regan, D. (1979) Separable aftereffects for changing size and for motion in depth: different neural mechanisms. *Vision Res.* 19, 727-732.
18. Regan, D. and Cynader, M. (1979) Neurons in cat parastriate cortex selectively sensitive to changing size: nonlinear interactions between two stimulating edges. *Vision Res.* 19, 699-711.



19. Campbell, F.W. and Robson, J.G. (1968) Application of Fourier analysis to the visibility of gratings. J. Physiol., Lond. 197, 551-566.
20. Pantle, A. and Sekuler, R. (1968) Size detecting mechanisms in human vision. Science 162, 1146-1148.  
Blakemore, C. and Campbell, F.W. (1969) On the existence of neurons in the human visual system selectively sensitive to the orientation and size of retinal images. J. Physiol., Lond. 203, 237-260.  
Pantle, A. (1974) Visual information processing of complex images. Report AMRL-TR-74-43, Aerospace Med. Res. Lab., Aerospace Med. Div. Air Force Syst. Command, Wright-Patterson, OH45433.
21. Sachs, M.B., Nachmias, J. and Robson, J.G. (1971) Spatial frequency channels in human vision. J. opt. Soc. Amer. 61, 1176-1186.
22. Richards, W. and Polit, A. (1974) Texture matching. Kybernetik 16, 155-162.
23. Kulikowski, J.J. and King-Smith, P.E. (1973) Spatial arrangement of line, edge, and grating detectors revealed by subthreshold summation. Vision Res. 13, 1455-1478.
24. Regan, D., Silver, R. and Murray, T.J. (1977) Visual acuity and contrast sensitivity in multiple sclerosis: hidden visual loss. Brain 100, 563-579.
25. Regan, D. and Beverley, K.I. (1973) Some dynamic features of depth perception. Vision Res. 13, 2369-2373.
26. Regan, D. and Beverley, K.I. (1973) The dissociation of sideways movements from movements in depth: psychophysics. Vision Res. 13, 2403-2415.
27. de Valois, K.K. (1977) Spatial frequency adaptation can enhance contrast sensitivity. Vision Res. 17, 1057-1065.
28. Giffin, F. and Mitchell, D.E. (1978) The rate of recovery of vision after early monocular deprivation in kittens. J. Physiol. 274.

29. Regan, D. and Beverley, K.I. Binocular and monocular stimuli for motion in depth: changing-disparity and changing-size feed the same motion-in-depth stage. Vision Res., 1979, 19, 1331-1342.
30. Regan, D. and Beverley, K.I. Visual responses to changing size and to sideways motion for different directions of motion in depth: linearization of visual responses. J. opt. Soc. Am., 1980, 11, 1289-1296.
31. Beverley, K.I. and Regan, D. Temporal selectivity of changing-size channels. J. opt. Soc. Am., 1980, 11, 1375-1377.
32. Koenderink, J.J. and van Doorn, A.J. Local structure of movement parallax of the plane. J. opt. Soc. Am., 1976, 66, 717-723.
33. Koenderink, J.J. and van Doorn, A.J. Exterospecific component of the motion parallax field. J. opt. Soc. Am., 1981, 71, 953-957.  
Llewellyn, K.R. Visual guidance of locomotion. J. Exp. Psych., 1971, 91, 245-261.
34. Regan, D. and Beverley, K.I. How do we avoid confounding the direction we are looking and the direction we are moving? Science, 1982, 215, 194-196.
35. Beverley, K.I. and Regan, D. Texture changes versus size changes as stimuli for motion in depth. Vision Res., in press.
36. Regan, D. and Cynader, M. Neurons in cat visual cortex tuned to the direction of motion in depth: effect of stimulus speed. Invest. Ophthalmol. Vis. Sci., 1982, 22, 535-550.
37. Cynader, M. and Regan, D. Neurons in cat visual cortex tuned to the direction of motion in depth: effect of positional disparity. Vision Res., 1982, 22, 967-82.
38. Regan, D. Visual information channeling in normal and disordered vision. Psych. Rev., 1982, 89, 407-444.



39. Regan, D. and Beverley, K.I. Psychophysics of visual flow patterns and motion in depth. Festschrift for Prof. I. Köhler, 1983, in press.
40. Beverley, K.I. and Regan, D. Device for measuring the precision of eye-hand coordination when tracking changing size. Aviation, Space & Environ. Med., 1980, 51, 688-693.
41. Kruk, R., Regan, D., Beverley, K.I. and Longridge, T. Correlations between visual test results and flying performance on the Advanced Simulator for Pilot Training (ASPT). Aviation, Space & Environ. Med., 1981, 52, 455-460.
42. Kruk., R., Regan, D., Beverley, K.I. and Longridge, T. Correlations between visual test results and flying performance on the Advanced Simulator for Pilot Training (ASPT) - II. Human Factors, in press.

Books

Regan, D. Evoked potentials in psychology, sensory physiology and clinical medicine. London: Chapman & Hall; New York: Wiley, 1972. 328 pp. Rpt. 1975.

Regan, D. The visual perception of motion. Oxford Psychology Series. Oxford University Press, in preparation.

Papers

1. Regan, D. Some characteristics of average steady-state and transient responses evoked by modulated light. Electroenceph. clin. Neurophysiol., 1966, 20, 238-248.
2. Regan, D. An apparatus for the correlation of evoked potentials and repetitive stimuli. Med. biol. Engng., 1966, 4, 168-177.
3. Regan, D. An effect of stimulus colour on average steady-state potentials evoked in man. Nature, 1966, 210, 1056-1057.
4. Regan, D. A high frequency mechanism which underlies visual evoked potentials. Electroenceph. clin. Neurophysiol., 1968, 25, 231-237.
5. Regan, D. Chromatic adaptation and steady-state evoked potentials. Vision Res., 1968, 8, 149-158.
6. Regan, D. Evoked potentials and sensation. Perception & Psychophysics, 1968, 4, 347-350.
7. Regan, D. Evoked potentials and colour vision. 7th ISCERG Symp., Istanbul (1969), publ. by University of Istanbul (1971), pp. 37-50.
8. Regan, D. Chapters 3 & 4 in D. M. MacKay (Ed.), Evoked potentials as indicators of sensory information processing. Neurosci. Res. Bull., 1969, 7, No. 3.
9. Regan, D. & Heron, J.R. Clinical investigation of lesions of the visual pathway: a new objective technique. J. Neurol. Neurosurg. Psychiat., 1969, 32, 479-483.
10. Tweel, L.H. van der, Regan, D. & Spekreijse, H. Some aspects of potentials evoked by changes in spatial brightness contrast. 7th ISCERG Symp., Istanbul (1969), publ. by University of Istanbul (1971), pp. 1-11.
11. Regan, D. Evoked potential and psychophysical correlates of changes in stimulus colour and intensity. Vision Res., 1970, 10, 163-178.
12. Regan, D. Objective method of measuring the relative spectral luminosity curve in man. J. opt. Soc. Am., 1970, 60, 856-859.
13. Regan, D. & Heron, J.R. Simultaneous recording of visual evoked potentials from the left and right hemispheres in migraine. In A.L. Cochrane (Ed.), Background to migraine. London: Heinemann, 1970, 66-77.
14. Regan, D. & Cartwright, R.F. A method of measuring the potentials evoked by simultaneous stimulation of different retinal regions. Electroenceph. clin. Neurophysiol., 1970, 28, 314-319.
15. Regan, D. & Spekreijse, H. Electrophysiological correlate of binocular depth perception in man. Nature, 1970, 255, 92-94.
16. Regan, D. & Sperling, H.G. A method of evoking contour-specific scalp potentials by chromatic checkerboard patterns. Vision Res., 1971, 11, 173-176.

17. Regan, D. & Tyler, C.W. Wavelength-modulated light generator. Vision Res., 1971, 11, 43-56.
18. Regan, D. & Tyler, C.W. Some dynamic features of colour vision. Vision Res., 1971, 11, 1307-1324.
19. Regan, D. & Tyler, C.W. Temporal summation and its limit for wavelength changes: an analog of Bloch's law for color vision. J. opt. Soc. Am., 1971, 61, 1414-1421.
20. Regan, D. & Richards, W. Independence of evoked potentials and apparent size. Vision Res., 1971, 11, 679-684.
21. Regan, D. Evoked potentials to changes in the chromatic contrast and luminance contrast of checkerboard stimulus patterns. In G.B. Arden (Ed.), The visual system. New York: Plenum, 1972.
22. Regan, D. Evoked potentials to changes in chromatic contrast. Proc. GAIN Symp. on EPs to spatial contrast. Trace, 1972, 6, 20-28.
23. Regan, D. Cortical evoked potentials. Adv. Behav. Biol., 1972, 5, 177-192.
24. Spekreijse, H., van der Tweel, L.H. & Regan, D. Interocular sustained suppression: correlations with evoked potential amplitude and distribution. Vision Res., 1972, 12, 521-526.
25. Milner, B.A., Regan, D. & Heron, J.R. Theoretical models of the generation of steady-state evoked potentials, their relation to neuroanatomy and their relevance to certain clinical problems. Advances Med. & Biol., 1972, 24, 157-169.
26. Regan, D. Parallel and sequential processing of visual information in man: investigation by evoked potential recording. In Photophysiology, Vol. 8. New York: Academic, 1973, 185-208.
27. Regan, D. An evoked potential correlate of colour: evoked potential findings and single-cell speculations. Vision Res., 1973, 13, 1933-1941.
28. Regan, D. Evoked potentials specific to spatial patterns of luminance and colour. Vision Res., 1973, 13, 2381-2402.
29. Regan, D. Rapid objective refraction using evoked brain potentials. Invest. Ophthalmol., 1973, 12, 669-679.
30. Regan, D. & Richards, W. Brightness contrast and evoked potentials. J. opt. Soc. Am., 1973, 63, 606-611.
31. Regan, D. & Beverley, K.I. Disparity detectors in human depth perception: evidence for directional selectivity. Science, 1973, 181, 877-879.
32. Regan, D. & Beverley, K.I. Some dynamic features of depth perception. Vision Res., 1973, 13, 2369-2379.
33. Regan, D. & Beverley, K.I. The dissociation of sideways movements from movements in depth: psychophysics. Vision Res., 1973, 13, 2403-2415.
34. Beverley, K.I. & Regan, D. Evidence for the existence of neural mechanisms selectively sensitive to the direction of movement in space. J. Physiol., 1973, 235, 17-29.
- 34a. Beverley, K.I. & Regan, D. Selective adaptation in stereoscopic depth perception. J. Physiol., 1973, 232, 40-41P.
35. Regan, D. & Beverley, K.I. Relation between the magnitude of flicker sensation and evoked potential amplitude in man. Perception, 1973, 2, 61-65.
36. Regan, D. & Beverley, K.I. Electrophysiological evidence for the existence of neurones sensitive to the direction of depth movement. Nature, 1973, 246, 504-506.

37. Richards, W. & Regan, D. A stereo field map with implications for disparity processing. Invest. Ophthalmol., 1973, 12, 904-909.
38. Cartwright, R.F. & Regan, D. Semi-automatic, multi-channel Fourier analyser for evoked potential analysis. Electroenceph. clin. Neurophysiol., 1974, 36, 547-550.
39. Regan, D. Electrophysiological evidence for colour channels in human pattern vision. Nature, 1974, 250, 437-439.
40. Regan, D. & Spekreijse, H. Evoked potential indications of colour blindness. Vision Res., 1974, 14, 89-95.
41. Heron, J.R., Regan, D. & Milner, B.A. Delay in visual perception in unilateral optic atrophy after retrobulbar neuritis. Brain, 1974, 97, 69-78.
42. Beverley, K.I. & Regan, D. Temporal integration of disparity information in stereoscopic perception. Exp. Brain Res., 1974, 19, 228-232.
43. Beverley, K.I. & Regan, D. Visual sensitivity to disparity pulses: evidence for directional selectivity. Vision Res., 1974, 14, 357-361.
44. Regan, D. Visually evoked potential methods with clinical applications. Proc. 11th ISCERG Symp., Bad Neuheim (1973). Docum. Ophthal., Series 4, 1974, 285-301.
45. Milner, B.A., Regan, D. & Heron, J.R. Differential diagnosis of multiple sclerosis by visual evoked potential recording. Brain, 1974, 97, 755-772.
46. Regan, D. Colour coding of pattern responses in man investigated by evoked potential feedback and direct plot techniques. Vision Res., 1975, 15, 175-183.
47. Heron, J.R., Milner, B.A. & Regan, D. Measurement of acuity variations within the central visual field caused by neurological lesions. J. Neurol. Neurosurg. Psychiat., 1975, 38, 356-362.
48. Regan, D., Schellart, N.A.M., Spekreijse, H. & van den Berg, T.J.T.P. Photometry in goldfish by electrophysiological recording. Vision Res., 1975, 15, 799-807.
49. Beverley, K.I. & Regan, D. The relation between discrimination and sensitivity in the perception of motion in depth. J. Physiol., 1975, 249, 387-398.
50. Regan, D. Recent advances in electrical recording from the human brain. Nature (review article), 1975, 253, 401-407.
51. Regan, D., Milner, B.A. & Heron, J.R. Delayed visual perception and delayed visual evoked potentials in the spinal form of multiple sclerosis and in retrobulbar neuritis. Brain, 1976, 99, 43-66.
52. Regan, D., Varney, P., Purdy, J. & Kraty, N. Visual field analyser: assessment of delay and temporal resolution of vision. Med. & Biol. Engng., 1976, 14, 8-14.
53. Regan, D. Latencies of evoked potentials to flicker and to pattern speedily estimated by simultaneous stimulation method. Electroenceph. clin. Neurophysiol., 1976, 40, 654-660.
54. Galvin, R.J., Regan, D. & Heron, J.R. A possible means of monitoring the progress of demyelination in multiple sclerosis: effect of body temperature on visual perception of double light flashes. J. Neurol. Neurosurg. Psychiat., 1976, 39, 861-865.
55. Galvin, R.J., Regan, D. & Heron, J.R. Impaired temporal resolution of vision after acute retrobulbar neuritis. Brain, 1976, 99, 255-268.
56. Regan, D. Fourier analysis of evoked potentials: some methods based on Fourier analysis. In J.E. Desmedt (Ed.), Visual evoked potentials in man: new developments. Oxford: Oxford University Press, 1977, 110-117.

57. Regan, D. Rapid methods for refracting the eye and for assessing visual acuity in amblyopia, using steady-state visual evoked potentials. In J.E. Desmedt (Ed.), Visual evoked potentials in man: new developments. Oxford: Oxford University Press, 1977, 418-426.
58. Regan, D. Evoked potential indications of the processing of pattern, colour, and depth information. In J.E. Desmedt (Ed.), Visual evoked potentials in man: new developments. Oxford: Oxford University Press, 1977, 234-249.
59. Regan, D., Milner, B.A. & Heron, J.R. Slowing of visual signals in multiple sclerosis, measured psychophysically and by steady-state evoked potentials. In J.E. Desmedt (Ed.), Visual evoked potentials in man: new developments. Oxford: Oxford University Press, 1977, 461-469.
60. Regan, D. Speedy assessment of visual acuity in amblyopia by the evoked potential method. Ophthalmologica, 1977, 175, 159-164.
61. Regan, D. & Spekreijse, H. Auditory-visual interactions and the correspondence between perceived auditory space and perceived visual space. Perception, 1977, 6, 133-138.
62. Galvin, R.J., Heron, J.R. & Regan, D. Subclinical optic neuropathy in multiple sclerosis. Arch. Neurol., 1977, 34, 666-670.
63. Regan, D. Steady state evoked potentials. Proc. Symp. Electrophysiological Techniques in Man. J. opt. Soc. Am., 1977, 67, 1475-1489.
64. Regan, D. & Milner, B.A. Objective perimetry by evoked potential recording: limitations. Electroenceph. clin. Neurophysiol., 1978, 44, 393-397.
65. Regan, D., Silver, R. & Murray, T.J. Visual acuity and contrast sensitivity in multiple sclerosis: hidden visual loss. Brain, 1977, 100, 563-579.
66. Regan, D. & Beverley, K.I. Looming detectors in the human visual pathway. Vision Res., 1978, 18, 415-421.
67. Cynader, M. & Regan, D. Neurones in cat parastriate cortex sensitive to the direction of motion in three-dimensional space. J. Physiol., 1978, 274, 549-569.
68. Regan, D. & Beverley, K.I. Illusory motion in depth: aftereffect of adaptation to changing size. Vision Res., 1978, 18, 209-212.
69. Hillyard, S.A., Picton, T.W. & Regan, D. Sensation, perception and attention: analysis using ERPs. In E. Callaway, P. Tueting & S.H. Koslow (Eds.), Event-related brain potentials in man. New York: Academic, 1978, 223-321.
70. Regan, D. Assessment of visual acuity by evoked potential recording: ambiguity caused by temporal dependence of spatial frequency selectivity. Vision Res., 1978, 18, 439-445.
71. Regan, D., Murray, T.J. & Silver, R. Effect of body temperature on visual evoked potential delay and visual perception in multiple sclerosis. J. Neurol. Neurosurg. Psychiat., 1977, 40, 1083-1091.
72. Arden, G.B., Bodis-Wollner, I., Halliday, A.M., Jeffreys, A., Kulikowski, J.J., Spekreijse, H. & Regan, D. Methodology of patterned visual stimulation. In J.E. Desmedt (Ed.), Visual evoked potentials in man: new developments. Oxford: Oxford University Press, 1977, 3-15.
73. Regan, D. Investigations of normal and defective colour vision by evoked potential recording. Mod. Probl. Ophthal., 1978, 19, 19-28.
74. Regan, D. Visual evoked potentials and visual perception in multiple sclerosis. Proc. San Diego Biomed. Symp., Vol. 16. New York: Academic, 1977, 87-95.

75. Regan, D. New methods for neurological assessment: overview. Proc. San Diego Biomed. Symp., Vol. 16. New York: Academic, 1977, 55-62.
76. Regan, D., Beverley, K.I. & Cynader, M. Stereoscopic depth channels for position and for motion. In S.J. Cool & E.L. Smith (Eds.), Frontiers in visual science. New York: Springer-Verlag, 1978, 351-372.
77. Regan, D. Evoked potentials in basic and clinical research. In A. Rémond (Ed.), EEG informatics: a didactic review of methods and applications of EEG data processing. Amsterdam: Elsevier, 1977, 319-346.
78. Regan, D. Colour and contrast. In H. Spekreijse & L.H. van der Tweel (Eds.), Spatial contrast: report of a workshop. Pub. for Netherlands Royal Academy of Sciences. Amsterdam: North-Holland, 1977, 75-79.
79. Regan, D., Beverley, K.I. & Cynader, M. Stereoscopic subsystems for position in depth and for motion in depth. Proc. R. Soc. Lond. B, 1979, 204, 485-501.
80. Regan, D. & Tansley, B.W. Selective adaptation to frequency-modulated tones: evidence for an information-processing channel selectively sensitive to frequency changes. J. acoust. Soc. Am., 1979, 65, 1249-1257.
81. Regan, D. & Beverley, K.I. Visually-guided locomotion: psychophysical evidence for a neural mechanism sensitive to flow patterns. Science, 1979, 205, 311-313.
82. Beverley, K.I. & Regan, D. Separable aftereffects of changing-size and motion-in-depth: different neural mechanisms? Vision Res., 1979, 19, 727-732.
83. Beverley, K.I. & Regan, D. Visual perception of changing size: the effect of object size. Vision Res., 1979, 19, 1093-1104.
84. Regan, D. & Cynader, M. Neurons in area 18 of cat visual cortex selectively sensitive to changing size: nonlinear interactions between responses to two edges. Vision Res., 1979, 19, 699-711.
85. Regan, D. New visual tests in multiple sclerosis. In H.S. Thompson (Ed.), Topics in neuro-ophthalmology. Baltimore: Williams & Wilkins, 1980, 219-242.
86. Regan, D. & Beverley, K.I. Binocular and monocular stimuli for motion-in-depth: changing-disparity and changing-size inputs feed the same motion-in-depth stage. Vision Res., 1979, 19, 1331-1342.
87. Regan, D., Beverley, K.I. & Cynader, M. The visual perception of motion in depth. Sci. Am., 1979, 241, 136-151.
88. Regan, D. Detection and quantification of neuroophthalmological abnormalities using psychophysical measures of visual delay and temporal resolution. In S. Sokol (Ed.), Electrophysiology and psychophysics: their use in ophthalmic diagnosis. Intnl. Ophthal. Clinics. Boston: Little, Brown, 1980, 185-204.
89. Regan, D. Visual psychophysical tests in multiple sclerosis as an aid to diagnosis, localization of pathology, and assessment of experimental therapy. In Clinical applications of visual psychophysics (Proc. NAS/NRC Symp.) New York: Cambridge University Press, 1981.
90. Tansley, B.W., Regan, D. & Suffield, J.B. Measurement of the sensitivities of information processing channels for frequency change and for amplitude change by a titration method. Can. J. Psychol., 1982, 36,
91. Beverley, K.I. & Regan, D. Visual sensitivity to the shape and size of a moving object: implications for models of object perception. Perception, 1980, 9, 151-160.
92. Regan, D., Whitlock, J., Murray, T.J. & Beverley, K.I. Orientation-specific losses of contrast sensitivity in multiple sclerosis. Invest. Ophthalmol. Vis. Sci., 1980, 19, 324-328.

93. Regan, D. & Beverley, K.I. Visual responses to changing size and to sideways motion for different directions of motion in depth: linearization of visual responses. J. opt. Soc. Am., 1980, 11, 1289-1296.
94. Regan, D. Control system and physiological monitoring applications of steady-state evoked potentials. In F.E. Gomer (Ed.), Biocybernetic applications for military systems. DARPA Conf., Chicago, 1978. St. Louis: McDonnell-Douglas. Report MDC E2191, 1980, pp. 175-202.
95. Tansley, B.W. & Regan, D. Separate auditory channels for unidirectional frequency modulation and unidirectional amplitude modulation. Sensory Processes, 1979, 3, 132-140.
96. Regan, D. & Beverley, K.I. Motion sensitivity measured by a psychophysical linearizing technique. J. opt. Soc. Am., 1981, 71, 958-965.
97. Regan, D. Electrical responses evoked from the human brain. Sci. Am., 1979, 241, 134-146.
98. Beverley, K.I. & Regan, D. Device for measuring the precision of eye-hand coordination when tracking changing size. Aviat. Space & Environ. Med., 1980, 51, 688-693.
99. Raymond, J., Regan, D. & Murray, T.J. Abnormal adaptation of visual contrast sensitivity in multiple sclerosis patients. Can. J. Neurol. Sci., 1981, 8, 221-234.
100. Noseworthy, J., Miller, J., Murray, T.J. & Regan, D. Auditory brainstem responses in postconcussion syndrome. Arch. Neurol., 1981, 38, 275-278.
101. Regan, D., Raymond, J., Ginsburg, A. & Murray, T.J. Contrast sensitivity, visual acuity and the discrimination of Snellen letters in multiple sclerosis. Brain, 1981, 104, 333-350.
102. Regan, D. Speedy evoked potential methods for assessing vision in normal and amblyopic eyes: pros and cons. Vision Res., 1980, 20, 265-269.
103. Petersik, J.T., Beverley, K.I. & Regan, D. Contrast sensitivity of the changing-size channel. Vision Res., 1981, 21, 829-832.
104. Petersik, J.T., Regan, D. & Murray, T.J. Double-flash thresholds as a function of field size in multiple sclerosis. In preparation.
105. Beverley, K.I. & Regan, D. Temporal selectivity of changing-size channels. J. opt. Soc. Am., 1980, 11, 1375-1377.
106. Beverley, K.I. & Regan, D. Adaptation to incomplete flow patterns: no evidence for "filling-in" the perception of flow patterns. Perception, 1982, 11,
107. Regan, D. Evoked potential studies of visual perception. Can. J. Psychol., 1981, 35, 77-112.
108. Cynader, M. & Regan, D. Neurons in cat visual cortex tuned to the direction of motion in depth: effect of positional disparity. Vision Res., 1982, 22, 967-982.
109. Regan, D. & Cynader, M. Neurons in cat visual cortex tuned to the direction of motion in depth: effect of stimulus speed. Invest. Ophthalmol. Vis. Sci., 1982, 22, 535-550.
110. Regan, D. Electrophysiology and psychophysics of motion in depth. Proc. 18th ISCERG Symp., Amsterdam, 1981. Docum. Ophthal., Proc. Series, 1981, 27, 271-281.
111. Regan, D., Regal, D.M. & Tibbles, J.A.R. Comparison of evoked potentials in a visually-disordered infant and his normally-sighted twin. Electroenceph. clin. Neurophysiol., 1982,
112. Regan, D. Visual information channeling in normal and disordered vision. Psych. Rev., 1982, 89, 407-444.

113. Regan, D. Psychophysical tests of vision and hearing in patients with multiple sclerosis. In S.G. Waxman & J.M. Ritchie (Eds.), Demyelinating disease: Basic and clinical electrophysiology. Proc. Vail Conf. MS Soc. of USA. New York: Raven, 1981, 217-237.
114. Kruk, R., Regan, D., Beverley, K.I. & Longridge, T. Correlations between visual test results and flying performance on the Advanced Simulator for Pilot Training (ASPT). Aviat. Space & Environ. Med., 1981, 52, 455-460.
115. Quine, D.B., Regan, D. & Murray, T.J. Delayed auditory tone perception in multiple sclerosis. J. Neurol. Sci., submitted.
116. Quine, D.B., Regan, D., Beverley, K.I. & Murray, T.J. Multiple sclerosis patients experience hearing loss specifically for changes of tone frequency: A possible cause of problems in understanding speech. Arch. Neurol., submitted.
117. Regan, D., Kruk, R., Beverley, K.I. & Longridge, T. The relevance of the channel theory of vision for the design of simulator imagery. Proc. Image II Conf., Arizona, 1981, 307-344.
118. Regan, D. Comparison of transient and steady-state methods. Proc. N.Y. Acad. Sci. 1982, 388, 46-71.
119. Regan, D. Binocular vision. In Encyclopaedia of Physics. Pergamon, 1982.
120. Regan, D. & Beverley, K.I. How do we avoid confounding the direction we are looking with the direction we are moving? Science, 1982, 215, 194-196.
121. Kaufman, L. & Regan, D. Visual perception of complex motion. In Handbook of vision, in press.
122. Regan, D. Human visual evoked potentials. In T. Picton (Ed.), Handbook of electrophysiology: Human event-related potentials. Amsterdam: Elsevier, 1983.
123. Kruk, R., Regan, D., Beverley, K.I. & Longridge, T. Flying performance on the Advanced Simulator for Pilot Training and laboratory tests of vision. Human Factors, in press.
124. Regan, D. Psychophysical tests. In The visual system in demyelinating diseases. Publ. Belgian Ophthal. Soc., in press.
125. Regan, D. & Beverley, K.I. Visual fields described by contrast sensitivity, by acuity and by relative sensitivity to different orientations. Invest. Ophthalmol. Vis. Sci., 1982, in press.
126. Beverley, K.I. & Regan, D. Texture changes versus size changes as stimuli for motion in depth. Vision Res., in press.
127. Regan, D. & Beverley, K.I. Psychophysics of visual flow patterns and motion in depth. In Sensory experience, adaptation and perception. Hillsdale, N.J.: Erlbaum, in press.
128. Regan, D., Bartol, S., Murray, T.J. & Beverley, K.I. Spatial frequency discrimination in normal vision and in patients with multiple sclerosis. Brain, 1982, 105, 735-754.
129. Regan, D. Spatial frequency mechanisms in human vision: electrophysiological evidence. Vision Res., submitted.
130. Regan, D. Visual psychophysical tests in diagnosis of multiple sclerosis. In C.M. Poser (Ed.), Diagnostic criteria for multiple sclerosis. New York: Thieme-Stratton, in press.
131. Regan, D. Evoked potentials in diagnosis. In M. Swash & C. Kennard (Eds.), Scientific basis of clinical neurology. Edinburgh: Churchill Livingstone, in press.

132. Regan, D., Beverley, K.I. & Macpherson, H. Sinewave grating response in amblyopic children measured psychophysically and by evoked potential recording. Invest. Ophthalmol. Vis. Sci., submitted.
133. Regan, D. & Beverley, K.I. Visual fields for frontal plane motion and for changing size. Vision Res., submitted.
134. Quine, D.B., Regan, D. & Murray, T.J. Speech-like sounds: loss of discrimination in patients with multiple sclerosis and Friedrich's Ataxia. In preparation.
135. Kruk, R., Regan, D., Beverley, K.I. & Longridge, T. Visual tests predict flying performance in telemetry-tracked aircraft. In preparation.
136. Regan, D. & Burbeck, C.A. Temporal factors in color discrimination. J. opt. Soc. Am.
137. Regan, D., Beverley, K.I. & Macpherson, H. Proc. 2nd. Intnl. Evoked Potential Conf., Cleveland, 1982, in press.
138. Regan, D. & Beverley, K.I. Figure-ground discrimination by relative motion. J. opt. Soc. Am.
139. Regan, D. & Beverley, K.I. Relationship between spatial frequency discrimination and spatial frequency channels. J. opt. Soc. Am.

(e) LIST OF PROFESSIONAL PERSONNEL ASSOCIATED WITH THE RESEARCH EFFORT

D. Regan (Principal Investigator)

|                            |      |                            |                          |
|----------------------------|------|----------------------------|--------------------------|
| D.Sc.                      | 1974 | Science, Medicine          | London University        |
| Ph.D.                      | 1964 | Physics                    | Imperial College, London |
| M.Sc. D.I.C.               | 1958 | Physics (Technical Optics) | Imperial College, London |
| B.Sc. (Sp. Hons), A.R.C.S. | 1957 | Physics                    | Imperial College, London |

K. I. Beverley (Research Associate)

|       |      |                                 |                                 |
|-------|------|---------------------------------|---------------------------------|
| Ph.D. | 1974 | Communication &<br>Neuroscience | University of Keele,<br>England |
| B.Sc. | 1969 | Physics & Psychology            | University of Keele             |

R. Kruk (Graduate Student)

|             |      |                     |                        |
|-------------|------|---------------------|------------------------|
| M.A.        | 1979 | Psychology (Vision) | University of Manitoba |
| B.A. (Hons) | 1977 | Psychology          | University of Manitoba |



(f) INTERACTIONS

(1) Spoken papers at meetings and conferences, 1981-1982

Regan, D. & Cynader, M. Motion in depth neurons: effects of speed and disparity.  
ARVO, Sarasota, May 1981.

Regan, D. The relevance of channel theory for the design of simulator imagery.  
Image II Conference, Arizona, June 1981.

Regan, D. Comparison of transient and steady-state methods. New York Academy  
of Sciences, June 1981.

Regan, D. New thoughts on evoked potentials. Invited address to Second Intnl.  
Evoked Potentials Symposium, Cleveland, Ohio, October 1982.

Regan, D. The role of size changes and texture in motion perception. Assn. for  
Research in Vision & Ophthalmology annual meeting, Sarasota, May 1982.

In addition, D. Regan has given invited lectures at the following Military  
Establishments, Universities and Hospitals:

Universities of New York, M.I.T., Utah, Concordia (Montreal), Manitoba, McGill,  
Montreal Neurological Institute.

Williams AFB and MCAS Yuma, Arizona.

Alberta Heritage Foundation Visiting Professor and lecturing at the University  
of Calgary and Foothills Hospital.

(2) Consultative and Advisory Functions

Dr. T. Longridge of Williams AFB AFHRL and Mr. R. Kruk, Dr. K. Beverley  
and Dr. D. Regan of Dalhousie University are jointly carrying out a study of  
vision in pilots. Mr. Kruk has been carrying out visual measurements (including  
changing-size sensitivity and changing-size tracking performance) on trainee  
and experienced pilots at Williams AFB, and comparing these data with flying  
grades and simulator performance on formation flying. We are now liaising with  
Mr. J. Taylor of Yuma TACTS in order to extend the implications of our two  
studies on the Williams ASPT flight simulator to pilot performance in radar-tracked



DEPARTMENT OF PHYSIOLOGY AND BIOPHYSICS

George Hall, Halifax Infirmary, 530B Morris Street,

Dalhousie University

Halifax, Nova Scotia

Canada, B3J 1S6

72

aircraft. In particular, we are correlating individual differences in dynamic visual sensitivity with pilot performance in several flying tasks including air-to-air combat manoeuvres, low-level approach and weapons delivery and formation flight.

**(g) NEW DISCOVERIES, INVENTIONS OR PATENT DISCLOSURES STEMMING FROM THE RESEARCH SUPPORT**

There has been no further invention since the motion-in-depth tracking technique that we reported previously and was then patented by the U.S. Air Force.